



# Profiling of aerosol microphysical properties at several EARLINET/AERONET sites during the July 2012 ChArMEx/EMEP campaign

María José Granados-Muñoz<sup>1,2,a</sup>, Francisco Navas-Guzmán<sup>3</sup>, Juan Luis Guerrero-Rascado<sup>1,2</sup>, Juan Antonio Bravo-Aranda<sup>1,2</sup>, Ioannis Biniotoglou<sup>4</sup>, Sergio Nepomuceno Pereira<sup>5</sup>, Sara Basart<sup>6</sup>, José María Baldasano<sup>6</sup>, Livio Belegante<sup>4</sup>, Anatoli Chaikovsky<sup>7</sup>, Adolfo Comerón<sup>8</sup>, Giuseppe D'Amico<sup>9</sup>, Oleg Dubovik<sup>10</sup>, Luka Ilic<sup>11</sup>, Panos Kokkalis<sup>12</sup>, Constantino Muñoz-Porcar<sup>8</sup>, Slobodan Nickovic<sup>11,13</sup>, Doina Nicolae<sup>4</sup>, Francisco José Olmo<sup>1,2</sup>, Alexander Papayannis<sup>12</sup>, Gelsomina Pappalardo<sup>9</sup>, Alejandro Rodríguez<sup>8</sup>, Kerstin Schepanski<sup>14</sup>, Michaël Sicard<sup>8,15</sup>, Ana Vukovic<sup>16,13</sup>, Ulla Wandinger<sup>14</sup>, François Dulac<sup>17</sup>, and Lucas Alados-Arboledas<sup>1,2</sup>

<sup>1</sup>Dpt. Applied Physics, Faculty of Sciences, University of Granada, Fuentenueva s/n, 18071, Granada, Spain

<sup>2</sup>Andalusian Institute for Earth System Research (IISTA-CEAMA), Avda. del Mediterráneo s/n, 18006, Granada, Spain

<sup>3</sup>Institute of Applied Physics (IAP), University of Bern, Bern, Switzerland

<sup>4</sup>National Institute of R&D for Optoelectronics, Magurele, Ilfov, Romania

<sup>5</sup>Departamento de Física, ECT, Instituto de Ciências da Terra, IIFA, Universidade de Évora, Évora, Portugal

<sup>6</sup>Earth Sciences Department, Barcelona Supercomputing Center-Centro Nacional de Supercomputación, BSC-CNS, Barcelona, Spain

<sup>7</sup>Institute of Physics, National Academy of Sciences of Belarus, Minsk, Belarus

<sup>8</sup>Dept. of Signal Theory and Communications, Remote Sensing Lab. (RSLab), Universitat Politècnica de Catalunya, Barcelona, Spain

<sup>9</sup>Consiglio Nazionale delle Ricerche – Istituto di Metodologie per l'Analisi Ambientale (CNR-IMAA), Potenza, Italy

<sup>10</sup>Laboratoire d'Optique Atmosphérique, CNRS Université de Lille 1, Bat P5 Cite scientifique, 59655, Villeneuve d'Ascq Cedex, France

<sup>11</sup>Institute of Physics, University of Belgrade, Belgrade, Serbia

<sup>12</sup>National Technical University of Athens, Physics Department, Laser Remote Sensing Laboratory, Zografou, Greece

<sup>13</sup>South East European Virtual Climate Change Center, Republic Hydrometeorological Service, Belgrade, Serbia

<sup>14</sup>Leibniz Institute for Tropospheric Research Leipzig, Leipzig, Germany

<sup>15</sup>Ciències i Tecnologies de l'Espai – Centre de Recerca de l'Aeronàutica i de l'Espai/Institut d'Estudis Espacials de Catalunya (CTE-CRAE/IEEC), Universitat Politècnica de Catalunya, Barcelona, Spain

<sup>16</sup>Faculty of Agriculture, University of Belgrade, Belgrade, Serbia

<sup>17</sup>Laboratoire des Sciences du Climat et de l'Environnement (IPSL-LSCE), CEA-CNRS-UVSQ, CEA Saclay, Gif-sur-Yvette, France

<sup>a</sup>currently at: Table Mountain Facility, NASA/Jet Propulsion Laboratory, California Institute of Technology, Wrightwood, California, USA

Correspondence to: María José Granados Muñoz (mamunoz@jpl.nasa.gov)

Received: 5 August 2015 – Published in Atmos. Chem. Phys. Discuss.: 20 November 2015

Revised: 7 April 2016 – Accepted: 21 May 2016 – Published: 9 June 2016

**Abstract.** The simultaneous analysis of aerosol microphysical properties profiles at different European stations is made in the framework of the ChArMEx/EMEP 2012 field campaign (9–11 July 2012). During and in support of this campaign, five lidar ground-based stations (Athens, Barcelona, Bucharest, Évora, and Granada) performed 72 h of continuous lidar measurements and collocated and coincident sun-photometer measurements. Therefore it was possible to retrieve volume concentration profiles with the Lidar Radiometer Inversion Code (LIRIC). Results indicated the presence of a mineral dust plume affecting the western Mediterranean region (mainly the Granada station), whereas a different aerosol plume was observed over the Balkans area. LIRIC profiles showed a predominance of coarse spheroid particles above Granada, as expected for mineral dust, and an aerosol plume composed mainly of fine and coarse spherical particles above Athens and Bucharest. Due to the exceptional characteristics of the ChArMEx database, the analysis of the microphysical properties profiles' temporal evolution was also possible. An in-depth analysis was performed mainly at the Granada station because of the availability of continuous lidar measurements and frequent AERONET inversion retrievals. The analysis at Granada was of special interest since the station was affected by mineral dust during the complete analyzed period. LIRIC was found to be a very useful tool for performing continuous monitoring of mineral dust, allowing for the analysis of the dynamics of the dust event in the vertical and temporal coordinates. Results obtained here illustrate the importance of having collocated and simultaneous advanced lidar and sun-photometer measurements in order to characterize the aerosol microphysical properties in both the vertical and temporal coordinates at a regional scale. In addition, this study revealed that the use of the depolarization information as input in LIRIC in the stations of Bucharest, Évora, and Granada was crucial for the characterization of the aerosol types and their distribution in the vertical column, whereas in stations lacking depolarization lidar channels, ancillary information was needed. Results obtained were also used for the validation of different mineral dust models. In general, the models better forecast the vertical distribution of the mineral dust than the column-integrated mass concentration, which was underestimated in most of the cases.

## 1 Introduction

The influence of the atmospheric aerosol particles on the Earth's radiative forcing is still affected by a large uncertainty, as indicated in the AR5 report from the Intergovernmental Panel for Climate Change (IPCC, 2013). During past years, this uncertainty has been reduced from high to medium with respect to the data in the Fourth Assessment Report (AR4) of the IPCC (2007). However, atmospheric aerosol

still contribute to the largest uncertainty to the total radiative forcing estimate, even though the level of confidence in the effects of atmospheric aerosols has increased from low and medium to medium and high (for indirect and direct effects, respectively) (IPCC, 2013).

The difficulty in accurately determining atmospheric aerosol properties and their influence on the Earth's radiative forcing lies in their large spatial and temporal variability. Ground-based (active and passive) remote sensing techniques have proven to be quite robust and provide accurate results for atmospheric aerosol characterization (e.g., Nakajima et al., 1996; Dubovik and King, 2000; Mattis et al., 2004; Olmo et al., 2006). Nonetheless, they provide information about atmospheric aerosol properties on a local scale. Since regional analyses are highly important when analyzing the aerosol variability, several observational networks have been developed, namely, the GALION (Global Atmospheric Watch Aerosol Lidar Observation Network) lidar network, which includes EARLINET (European Aerosol Research Lidar Network, [www.earlinet.org](http://www.earlinet.org)) (Bösenberg et al., 2001; Pappalardo et al., 2014), MPLNET (Micro Pulse Lidar Network) (Welton et al., 2005), LALINET (Latin American Lidar Network, [www.lalinet.org](http://www.lalinet.org)) (Guerrero-Rascado et al., 2014), and ADNET (Asian Dust Network) (Shimizu et al., 2004) among others, and sun-photometer networks SKYNET (Skyradiometer network) (Takamura and Nakajima, 2004) and AERONET (Aerosol Robotic Network, <http://aeronet.gsfc.nasa.gov/>) (Holben et al., 1998).

In addition to the regional coverage, these networks can provide useful information on the vertical and temporal coordinates, if adequate measurement protocols are established. Information on the vertical structure of the aerosol is of high importance, since the atmospheric aerosol effects can be very different near the surface, within the boundary layer, and in the free troposphere. Estimates of radiative forcing are sensitive to the vertical distribution of aerosols (Claquin et al., 1998; Huang et al., 2009; Sicard et al., 2015) and the vertical information is required for accounting for the indirect effect (McCormick et al., 1993; Bréon, 2006). In addition, atmospheric aerosol can change the vertical profile of temperature and atmospheric stability, which in turn influences the wind speed profile within the lower atmosphere (Pérez et al., 2006a, b; Guerrero-Rascado et al., 2009; Choobari et al., 2014). Furthermore, continuous and/or regular measurements provided by the networks would allow us to analyze the temporal evolution and dynamics of the atmospheric aerosol particles, which will be very useful not only for accurately determining the radiative forcing, but also for improving the performance of numerical weather prediction (NWP) (e.g., Pérez et al., 2006a) and climatological models (Nabat et al., 2014, 2015).

Lidar systems are widely used to determine the vertical distribution of aerosols. There are already many regional studies on the vertical characterization of optical properties based on lidar systems (e.g., Papayannis et al., 2008). How-

ever, the characterization of the microphysical properties profiles is still not so straightforward, due to the complexity of the retrievals. Algorithms designed to combine lidar and sun-photometer measurements have been developed in order to overcome this difficulty, e.g., the Lidar Radiometer Inversion Code, LIRIC (Chaikovsky et al., 2008, 2012, 2016), and Generalized Aerosol Retrieval from Radiometer and Lidar Combined data, GARRLIC (Lopatin et al., 2013). The combination of simultaneous information about the aerosol vertical structure provided by the lidar system and the columnar properties provided by the sun photometer has proven to be a promising synergetic tool for this purpose. LIRIC, which is used in this study, has already provided interesting results about vertically resolved aerosol microphysical properties for selected case studies (Tsekeri et al., 2013; Wagner et al., 2013; Granados-Muñoz et al., 2014, 2016; Papayannis et al., 2014; Biniotoglou et al., 2015). The increasing number of stations performing these simultaneous measurements foreshadows an optimistic future concerning the increasing spatial coverage.

Regional studies in the Mediterranean region are of huge scientific interest since multiple studies indicate that aerosol radiative forcing over the Mediterranean region is one of the largest in the world (Lelieveld et al., 2002; IPCC, 2013). In this context, the ChArMEx (the Chemistry-Aerosol Mediterranean Experiment, <http://charmex.lscce.ipsl.fr/>) (Dulac, 2014) international project involving several Mediterranean countries aims at developing and coordinating regional research actions for a scientific assessment of the present and future state of the atmospheric environment in the Mediterranean basin, and of its impacts on the regional climate, air quality, and marine biogeochemistry. The ChArMEx project organized a field campaign between 25 June and 12 July 2012, in order to address interactions such as long-range transport and air quality, and aerosol vertical structure and sources. The period of the campaign falls within the ACTRIS (Aerosols, Clouds, and Trace Gases Research Infrastructure Network) summer 2012 campaign (8 June–17 July 2012) that aimed at giving support to both the ChArMEx and EMEP (European Monitoring and Evaluation Programme) (Espen Yttri et al., 2012) field campaigns. Within the ACTRIS summer 2012 campaign, the European lidar network (EARLINET) (Pappalardo et al., 2014) performed a controlled exercise of feasibility to demonstrate its potential to perform operational, coordinated measurements (Sicard et al., 2015). The exercise consisted of continuous lidar measurements during a 72 h period in July 2012 at different European sites. Most of those lidar data have been successfully assimilated by a regional particulate air quality model to improve 36 h operational aerosol forecasts in terms of both surface PM and aerosol optical depth (Wang et al., 2014).

Our study takes advantage of those continuous lidar measurements combined with simultaneous sun-photometer data to perform a characterization of the vertical distribution of

the aerosol microphysical properties at different European stations with LIRIC. The temporal evolution of the aerosol microphysical properties is also analyzed when the continuity of the inverted data is available. To our knowledge, it is the first time that the LIRIC algorithm has been applied in a continuous and automated way to retrieve simultaneous and continuous data acquired at different stations, proving the algorithm's ability to provide reliable information about microphysical properties with high spatial and temporal resolution. In addition, this exceptional aerosol observational database is used for the spatio-temporal evaluation of different regional mineral dust models.

## 2 Measurement strategy

During the summer of 2012, an intensive measurement campaign was performed in the framework of ChArMEx and EMEP in the Mediterranean basin at 12 ground-based lidar stations throughout Europe. The main aim of these measurements was to obtain an experimental vertically resolved database for investigating aerosol radiative impacts over the Mediterranean basin using 3-D regional climate models. The extensive lidar database acquired during this campaign combined with AERONET regular measurements represents a unique opportunity to evaluate the performance of LIRIC microphysical inversion retrieval during the event in both temporal and spatial (horizontal and vertical) coordinates, proving the utility of combined measurements and the potential of the LIRIC algorithm for routine aerosol microphysical properties measurements.

The measurement campaign consisted in 72 h of continuous and simultaneous lidar measurements performed at 12 European stations, with 11 of them participating in ACTRIS/EARLINET (Sicard et al., 2015). The measurement period started on 9 July at 06:00 UTC and lasted until 12 July 2012 at 06:00 UTC, coinciding with a forecast mineral dust event over the Mediterranean basin according to dust transport models.

The LIRIC algorithm requires lidar data in at least three different wavelengths and simultaneous AERONET retrievals in order to obtain the aerosol microphysical properties profiles. Therefore, to evaluate the performance of the LIRIC algorithm and characterize the distribution and temporal evolution of the aerosol microphysical properties during the event, only those stations where multiwavelength lidar data at three wavelengths and AERONET data were available for the period 9–11 July were selected. Those stations were Athens (AT), Barcelona (BA), Bucharest (BU), Évora (EV), and Granada (GR) (Fig. 1). The main characteristics of each station are included in Table 1.

All five stations are part of both EARLINET and AERONET networks. Thus, these five stations are equipped with at least a multiwavelength lidar and a sun photometer. Lidar systems in all these five stations emit and receive at

**Table 1.** Lidar and sun-photometer characteristics for the five stations considered in this study and depicted in Fig. 1. A more detailed description of the experimental sites and the lidar systems in every station can be found in the references included in the “Reference” column of the table.

Site	Latitude, longitude	Altitude (m a.s.l.)	Lidar characteristics			Sun-photometer characteristics channels (nm)	Reference
			Elastic channels (nm)	Raman channels (nm)	System name		
AT (Athens)	37.97° N, 23.77° E	200	355, 532, 1064	387, 407, 607	EOLE	340, 380, 440, 500, 675, 870, 1020, 1640	Kokkalis et al. (2012)
BA (Barcelona)	41.39° N, 2.17° E	115	355, 532, 1064	387, 407, 607	UPCLidar	440, 675, 870, 1020	Kumar et al. (2011)
BU (Bucharest)	44.35° N, 26.03° E	93	355, 532 parallel, 532 cross, 1064	387, 407, 607	RALI (LR313–D400)	340, 380, 440, 500, 675, 870, 1020	Nemuc et al. (2013)
EV (Évora)	38.57° N, 7.91° W	293	355, 532, 532 cross, 1064	387, 407, 607	PAOLI	340, 380, 440, 500, 675, 870, 1020, 1640	Preißler et al. (2011)
GR (Granada)	37.16° N, 3.61° W	680	355, 532 parallel, 532 cross, 1064	387, 407, 607	MULHACEN (LR321-D400)	340, 380, 440, 500, 675, 870, 1020	Guerrero-Rascado et al. (2009)



**Figure 1.** Stations where the LIRIC algorithm was applied during the ChArMEx/EMEP 2012 intensive measurement period on 9–11 July. Source: Google Earth.

least at three different wavelengths (355, 532, and 1064 nm), with the systems in Granada, Bucharest, and Évora including depolarization capabilities at 532 nm (Table 1). Depolarization information can be used in the retrieval of the aerosol microphysical properties profiles with LIRIC to distinguish between coarse spherical and coarse spheroid mode.

Stations are also equipped with collocated standard sun photometers CIMEL CE-318-4, used in the AERONET network. The AERONET retrieval algorithm provides atmospheric aerosol properties integrated into the atmospheric vertical column (Dubovik and King, 2000; Dubovik et al., 2006). The automatic tracking sun and sky scanning radiometer makes sun direct measurements with a 1.2° full field of view every 15 min at different nominal wavelengths, depending on the station (Table 1). These solar extinction measurements are used to compute aerosol optical depth ( $\tau_\lambda$ ) at each wavelength except for the 940 nm channel, which is

used to retrieve total column water vapor (or precipitable water) (Estellés et al., 2006; Pérez-Ramírez et al., 2012). The estimated uncertainty in computed  $\tau_\lambda$ , due primarily to calibration uncertainty, is around 0.01–0.02 for field instruments (which is spectrally dependent, with the larger errors in the UV) (Eck et al., 1999; Estellés et al., 2006).

### 3 Methodology

#### 3.1 Retrieval of aerosol properties from remote sensing measurements

The analysis of aerosol microphysical properties profiles is performed with the LIRIC algorithm. Details about the LIRIC retrieval algorithm and its physical basics can be found in previous studies (Chaikovsky et al., 2012, 2016; Kokkalis et al., 2013; Wagner et al., 2013; Granados-Muñoz et al., 2014, 2016; Perrone et al., 2014; Biniotoglou et al., 2015), but a brief description is included here for completeness. LIRIC provides profiles of atmospheric aerosol microphysical properties from atmospheric aerosol columnar optical and microphysical properties retrieved from direct sun and sky radiance measurements from the sun photometer using the AERONET code (version 2, level 1.5) (Dubovik and King, 2000; Dubovik et al., 2006) and measured lidar elastic backscatter signals at three different wavelengths (355, 532, and 1064 nm). If available, the 532 nm cross-polarized signal is also used. Raw lidar data used for this analysis have been prepared according to the EARLINET Single Calculus Chain (SCC), described in detail in D’Amico et al. (2015). From the combination of all these data, volume concentration profiles  $C_V(z_n)$  are obtained for fine and coarse aerosol particles, with a vertical resolution of 15 m in our case. The

use of the 532 nm cross-polarized lidar channel allows one to distinguish between spherical and non-spherical particles within the coarse fraction of the aerosol. The uncertainty in LIRIC retrievals associated with the input data is not yet well described, but the algorithm has proven to be very stable, and the variations in the output profiles associated with the user-defined input parameters are below 20 % (Granados-Muñoz et al., 2014).

### 3.2 Model description and validation strategy

Models of dust emission, transport, and deposition are used as a tool to understand the various aspects that control distributions and impacts of dust. While global models of the dust cycle are used to investigate dust at large scales and long-term changes, regional dust models are the ideal tool to study in detail the processes that influence dust distribution as well as individual dust events. The analysis of the aerosol microphysical properties with LIRIC using the ChArMEx comprehensive database was used here for the evaluation of a set of four regional mineral dust models. This model evaluation was performed for both the vertical and horizontal coordinates and the temporal evolution.

Firstly, the spatial distribution of the mineral dust was examined by using the experimental data from the five EARLINET/AERONET sites considered in the present study. Dust optical depth (at 550 nm) provided by four different regional mineral dust models (BSC-DREAM8b, NMMB/BSC-Dust, DREAM8-NMME, and the regional version of COSMO-MUSCAT) was used at this stage. Experimental data were used here just to corroborate the presence or non-presence of mineral dust at the different regions and periods indicated by the models.

The BSC-DREAM8b and DREAM8-NMME models are based on the Dust Regional Atmospheric Model (DREAM) originally developed by Nickovic et al. (2001). The main feature of the updated version of the model, BSC-DREAM8b (version 2), includes an eight-bin size distribution within the 0.1–10  $\mu\text{m}$  radius range according to Tegen and Lacis (1996), radiative feedbacks (Pérez et al., 2006a, b), and upgrades in its source mask (Basart et al., 2012). The BSC-DREAM8b model provides daily dust forecasts at the Barcelona Supercomputing Center-Centro Nacional de Supercomputación (BSC-CNS, 2016). The model has been extensively evaluated against observations (see, e.g., Basart et al., 2012). Recently, the DREAM8-NMME model (Vukovic et al., 2014), driven by the NCEP Nonhydrostatic Mesoscale Model on E-grid (Janjic et al., 2001), has provided daily dust forecasts available at the South East European Virtual Climate Change Center (SEEVCCC; <http://www.seevccc.rs/>).

The NMMB/BSC-Dust model (Pérez et al., 2011; Hausteine et al., 2012) is a regional to global dust forecast operational system developed and maintained at BSC-CNS. It is an online multi-scale atmospheric dust model designed and developed at BSC-CNS in collaboration with NOAA-

NCEP, the NASA Goddard Institute for Space Studies, and the International Research Institute for Climate and Society (IRI). The NMMB/BSC-Dust model includes a physically based dust emission scheme, which explicitly takes into account saltation and sandblasting processes. It includes an eight-bin size distribution and radiative interactions. The NMMB/BSC-Dust model has been evaluated at regional and global scales (Pérez et al., 2011; Hausteine et al., 2012; Gama et al., 2015).

The BSC-DREAM8b, NMMB/BSC-DDUST, and DREAM8-NMME models are participating in the World Meteorological Organization Sand and Dust Storm Warning Advisory and Assessment System (WMO SDS-WAS) Northern Africa-Middle East-Europe (NAMEE) Regional Center (<http://sds-was.aemet.es/>). Additionally, NMMB/BSC-Dust is the model that provides operational dust forecast in the first Regional Specialized Meteorological Center with activity specialization on Atmospheric Sand and Dust Forecast, the Barcelona Dust Forecast Center (BDFC; <http://dust.aemet.es/>).

On the other hand, COSMO-MUSCAT is an online coupled model system based on a different philosophy: COSMO is a non-hydrostatic and compressible meteorological model that solves the governing equations on the basis of a terrain-following grid (Schättler et al., 2008; Baldauf et al., 2011), whereas MUSCAT is a chemistry transport model that treats the atmospheric transport as well as chemical transformations for several gas-phase species and particle populations using COSMO output data (Knoth and Wolke, 1998; Wolke et al., 2012). More details about the COSMO-MUSCAT model can be found elsewhere (Schepanski et al., 2007, 2009; Heinold et al., 2009; Laurent et al., 2010; Tegen et al., 2013).

The spatial resolution, domain size, and initial and boundary conditions differ, in addition to the different physical parameterizations implemented in the models. Details on the individual mineral dust models and their respective model configurations evaluated here are summarized in Table 2.

In a further step, modeled mineral dust mass concentration profiles were compared with LIRIC output profiles in order to evaluate the model performance on the vertical coordinate. The temporal evolution of the modeled vertical profiles was evaluated in more detail only at Granada, which was the station most affected by the dust outbreak during the analyzed period, and thus provided a more extensive database. Since LIRIC provides volume concentration profiles, a conversion factor was needed to obtain mass concentration. This conversion factor was the density of the aerosol particles, namely 2.65  $\text{g cm}^{-3}$  for the coarse mode (1–10  $\mu\text{m}$ ) and 2.5  $\text{g cm}^{-3}$  (0.1–1  $\mu\text{m}$ ) for the fine mode (Pérez et al., 2006a, b). In addition, the initial vertical resolution of the different models and LIRIC was established to a common value of 100 m, in order to obtain a compromise between the loss of information from LIRIC and from the different models, following a similar procedure to that in Binietoglou et al. (2015).

**Table 2.** Summary of the main parameters of the mineral dust transport models used in this study.

	BSC-DREAM8b	NMMB/BSC-Dust	COSMO-MUSCAT	DREAM8-NMME
Institution	BSC-CNS	BSC-CNS	TROPOS	SEEVCCC/IPB
Meteorological driver	Eta/NCEP	NMMB/NCEP	COSMO	NMME/NCEP
Initial and boundary conditions	NCEP/FNL	NCEP/FNL	GME	ECMWF analysis data in 6 h intervals
Domain	30° W to 65° E and 0 to 65° N	30° W to 65° E and 0 to 65° N	30° W to 35° E and 0 to 60° N	221 × 251 points, 26° W, 62° E, 7, 57° N
Resolution	0.33° × 0.33°	0.33° × 0.33°	0.25° × 0.25°	0.2° × 0.2°
Vertical resolution	24 Eta layers	40 $\sigma$ -hybrid layers	41 $\sigma$ -hybrid layers	28 $\sigma$ -hybrid pressure levels
Radiation interaction	Yes	Not activated	Yes, online	No
Data assimilation	No	No	No	No

After this processing, mineral dust mass concentration profiles provided by the BSC-DREAM8b, NMMB/BSC-DUST, DREAM8-NMME, and COSMO-MUSCAT models were evaluated against LIRIC results in those cases when mineral dust was detected. For the comparison, the fine mode was assumed to be fine mineral dust since it is not possible to distinguish which part of the fine mode corresponds to dust or non-dust particles with LIRIC. This assumption may cause an overestimation of the mineral dust concentration that becomes more important in those cases with high concentrations of the fine mode (which was not the case in our study). Alternative methods, such as the POLIPHON (Polarization-lidar photometer networking) method, could be applied to overcome this difficulty (Mamouri and Ansmann, 2014), but this is beyond the scope of our study.

In our study, model output profiles were retrieved every 3 h and compared to LIRIC retrievals during the 3 analyzed days. Only daytime data are presented here (from 06:00 to 18:00 UTC) because of the limitations of LIRIC retrieval during night-time. Due to the difficulties of the models in correctly representing the convective processes occurring within the planetary boundary layer and PBL-free troposphere interactions and the photochemical reactions producing secondary aerosols at the considered resolution, the lowermost parts of LIRIC profiles (affected by these processes) were not considered in the comparison presented here. Only data between 2000 m a.s.l., which is the mean value of the PBL height during summer at Granada (Granados-Muñoz et al., 2012), and the highest value (up to between 5 and 6 km) provided by LIRIC were included in the comparisons.

In order to quantify the model agreement with the total dust load observed in the profiles, the integrated dust mass concentration from the different profiles was obtained by integrating the profiles between 2 km a.s.l. and the highest altitude value provided by LIRIC profiles.

The altitude of the center of mass of the dust column ( $C_m$ ) was also calculated according to Eq. (1), where  $z_{\min}$  and  $z_{\max}$  are 2 km and the highest altitude value provided by LIRIC,

respectively,

$$C_m = \frac{\int_{z_{\min}}^{z_{\max}} z_n C_{\text{mass}}(z_n) \cdot dz_n}{\int_{z_{\min}}^{z_{\max}} C_{\text{mass}}(z_n) \cdot dz_n} \quad (1)$$

Additional parameters used in the comparison between LIRIC and the model dust mass concentration profiles are the root mean square error (RMSE), the correlation coefficient ( $R$ ), the normalized mean bias (NMB), and the normalized mean standard deviation (NMSD), defined in Eqs. (2) to (5):

$$\text{RMSE} = \sqrt{\frac{1}{n} \sum_n (C_{\text{mass}}^{\text{LIRIC}}(z_n) - C_{\text{mass}}^{\text{model}}(z_n))^2} \quad (2)$$

$$R = \frac{\sum_n (C_{\text{mass}}^{\text{model}}(z_n) - \overline{C_{\text{mass}}^{\text{model}}})(C_{\text{mass}}^{\text{LIRIC}}(z_n) - \overline{C_{\text{mass}}^{\text{LIRIC}}})}{\sqrt{\sum_n (C_{\text{mass}}^{\text{model}}(z_n) - \overline{C_{\text{mass}}^{\text{model}}})^2} \sqrt{\sum_n (C_{\text{mass}}^{\text{LIRIC}}(z_n) - \overline{C_{\text{mass}}^{\text{LIRIC}}})^2}} \quad (3)$$

$$\text{NMB} = \frac{\overline{C_{\text{mass}}^{\text{model}}} - \overline{C_{\text{mass}}^{\text{LIRIC}}}}{\overline{C_{\text{mass}}^{\text{LIRIC}}}} \quad (4)$$

$$\text{NMSD} = \frac{\sigma_{\text{model}} - \sigma_{\text{LIRIC}}}{\sigma_{\text{LIRIC}}} \quad (5)$$

where  $n$  is the number of height levels;  $C_{\text{mass}}(z_n)$  is the dust mass concentration at each height level  $z_n$ , either for LIRIC or the models;  $\overline{C_{\text{mass}}}$  are mean values; and  $\sigma$  indicates the standard deviation.

A detailed comparison of BSC-DREAM8b, NMMB/BSC-DUST, and DREAM8-NMME (three out of the four models presented here) dust mass concentration profiles with LIRIC results was performed in Binietoglou et al. (2015) using additional stations and selected case studies for the period 2011–2013. However, due to the characteristics of the ChArMEx database this study goes a step further. To our knowledge, it is the first time that the different models have been evaluated at different stations using simultaneous data, thus providing information about the horizontal coordinate, following the evolution of a regional event. Additionally, a validation of

the mass concentration profile temporal evolution of a specific mineral dust event is presented for the first time.

## 4 Results

During the 72 h intensive measurement period, information from different models, platforms, and instrumentation was available. A detailed characterization of the situation above the Mediterranean basin during the campaign focusing on aerosol microphysical properties using the different resources available is presented in Sect. 4.1, followed by the model evaluation in Sect. 4.2.

### 4.1 Spatial–temporal characterization of aerosol microphysical properties during ChArMEx/EMEP 2012

#### 4.1.1 Ground-based column-integrated measurements

Column-integrated properties retrieved from the AERONET sun photometer are presented in Fig. 2. Figure 2a and b shows the time series of the  $\tau_{440\text{nm}}$  and AE(440–880 nm) for the selected five stations during the analyzed period, and mean values for each day and station are indicated in Table 3.

According to these data, the lowest values of  $\tau_{440\text{nm}}$  were measured at the Évora station during the whole period, with values below 0.18. The AE(440–880 nm) was close to 1, except in the early morning and late evening, when it decreased down to  $\sim 0.5$ . These values, together with the columnar volume size distributions observed in Fig. 2c, indicate a very low aerosol load, mostly related to aerosol from local sources, and no impact of the northern African aerosol plume forecast to arrive at the Iberian Peninsula. A decrease in the  $\tau_{440\text{nm}}$  value with time was observed at the Granada station, with maximum values reaching up to 0.40 on 9 July around 16:00 UTC. During 10 and 11 July,  $\tau_{440\text{nm}}$  values were between 0.10 and 0.20, except for the late afternoon of 10 July from 17:00 UTC, when the aerosol load decreased and  $\tau_{440\text{nm}}$  below 0.10 were observed. By contrast, values of the AE(440–870 nm) increased from 0.3 on 9 July up to 0.7 on 11 July, with maximum values on the late evening on 10 July (AE(440–870 nm) > 1). It is worth noting that the AE(440–870 nm) was below 0.5 during the whole period except for the late afternoon on 10 July, coinciding with the decrease in  $\tau_{440\text{nm}}$ , indicating a clear predominance of coarse particles (e.g., Pérez et al., 2006a; Basart et al., 2009; Valenzuela et al., 2014). The columnar volume size distributions for the different days agreed with these data. Data from 9 July show a very large coarse mode and a small contribution of fine particles. The contribution of fine particles was almost constant during the 3 days, whereas the coarse mode was decreasing with time. There was a predominance of the coarse mode during the whole period, with maximum values of  $0.13 \mu\text{m}^3 \mu\text{m}^{-2}$  during the first day. All these data are usually related to the presence of mineral dust in the station and

the temporal evolution of the analyzed properties clearly suggests a decrease in the mineral dust event intensity throughout the analyzed period and a possible mixing or aging of the mineral dust. At the Barcelona station no AERONET data were available on 9 July. During 10 and 11 July,  $\tau_{440\text{nm}}$  values were relatively high and quite constant (around 0.30) and the AE(440–870 nm) values were larger than 1.5, indicating a strong contribution of fine aerosol particles. In the columnar volume size distributions, similar values for the fine and coarse modes were observed on 10 July, but larger values of the fine mode were obtained on 11 July. Therefore, it can be inferred from these data that the impact of the northern African aerosol plume was almost negligible at this station.

In Athens and Bucharest the aerosol plume presented very different characteristics to those observed in the western region (Table 3). In this region, large  $\tau_{440\text{nm}}$  values (> 0.35) and large values of the AE(440–870 nm) suggested a situation with high aerosol load mainly composed of fine particles. At Athens both  $\tau_{440\text{nm}}$  and AE(440–870 nm) values were very constant during the 3 analyzed days, except for a slight decrease in the AE(440–870 nm) on 11 July (from  $\sim 1.70$  to  $\sim 1.30$ ). This is in agreement with the columnar volume size distributions (Fig. 3c), where a slight increase in the coarse mode was observed on 11 July when compared to 9 and 10 July. In the case of Bucharest,  $\tau_{440\text{nm}}$  was almost constant on 9 and 10 July (around 0.37), but increased on 11 July (over 0.60). The AE(440–870 nm) was almost constant around 1.10 during the 3 days, indicating a balanced presence of coarse and fine particles despite the increase in the aerosol load during 11 July. The columnar volume size distributions were very similar to those of Athens on 9 and 10 July, but a larger presence of fine particles was observed here on 11 July. According to these sun-photometer data, the aerosol plume over this region was not composed of mineral dust particles, even though low concentrations of mineral dust might have been advected over Athens on 11 July.

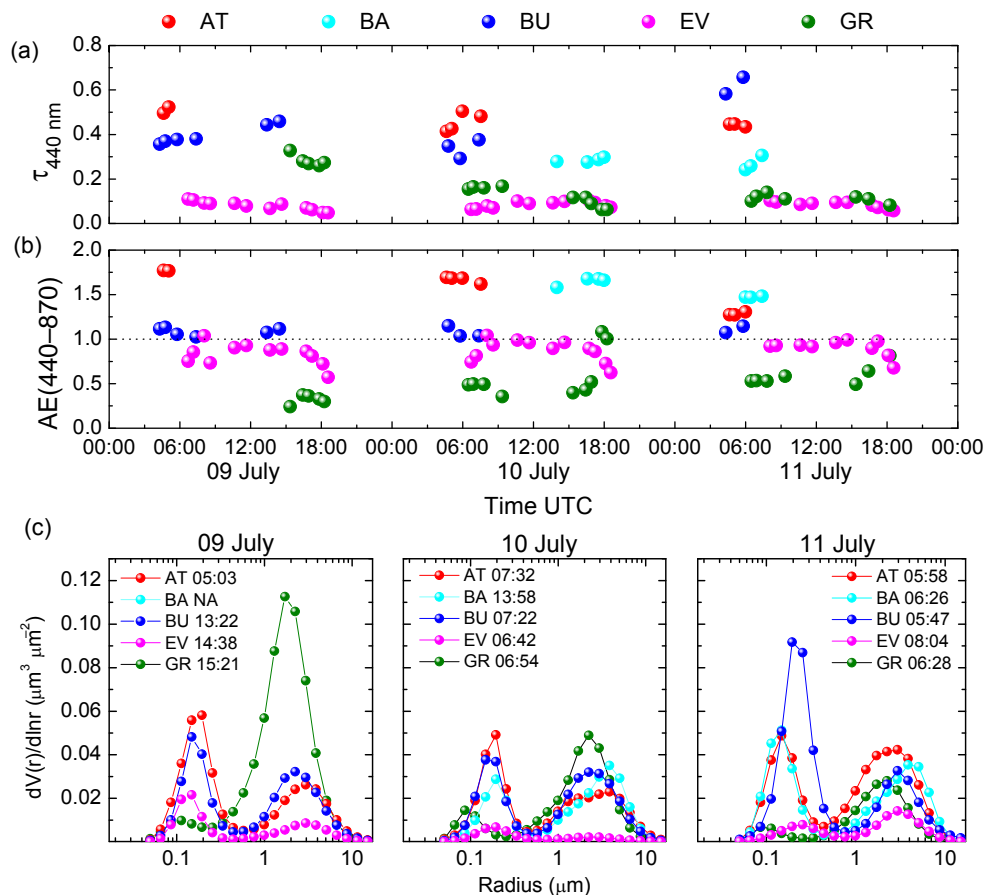
#### 4.1.2 Aerosol vertical distribution

Figure 3 shows the time series of the lidar range-corrected signal (RCS) in arbitrary units at 532 nm (at 1064 nm in Athens) for the 72 h period at the different stations. From these plots, it is clearly observed that at Barcelona and Évora the aerosol load was mainly confined within the planetary boundary layer, and the time series reveal the evolution of the planetary boundary layer height, even though at Barcelona some aerosol layers are observed in the free troposphere. Therefore, it is expected that most of the aerosol particles are of local origin. However, at the rest of the stations a more complex vertical structure was observed and the presence of a lofted aerosol layer reaching up to 6 km a.s.l. at some periods indicated the advection of different aerosol types.

The aerosol microphysical properties profiles retrieved with LIRIC for different periods at the different stations are shown in Fig. 4. That is, the volume concentration profiles

**Table 3.**  $\tau_{440\text{ nm}}$  and AE(440–870 nm) daily mean values ( $\pm$  standard deviation) at the five stations on 9, 10, and 11 July 2012.

Site	9 July		10 July		11 July	
	$\tau_{440\text{ nm}}$	AE(440–870 nm)	$\tau_{440\text{ nm}}$	AE(440–870 nm)	$\tau_{440\text{ nm}}$	AE(440–870 nm)
AT	$0.51 \pm 0.02$	$1.76 \pm 0.01$	$0.45 \pm 0.05$	$1.67 \pm 0.03$	$0.44 \pm 0.01$	$1.28 \pm 0.02$
BA	NA	NA	$0.28 \pm 0.01$	$1.65 \pm 0.05$	$0.27 \pm 0.03$	$1.47 \pm 0.01$
BU	$0.40 \pm 0.04$	$1.08 \pm 0.04$	$0.34 \pm 0.04$	$1.07 \pm 0.06$	$0.62 \pm 0.05$	$1.10 \pm 0.05$
EV	$0.08 \pm 0.02$	$0.82 \pm 0.12$	$0.08 \pm 0.01$	$0.87 \pm 0.12$	$0.08 \pm 0.02$	$0.90 \pm 0.09$
GR	$0.28 \pm 0.03$	$0.32 \pm 0.05$	$0.12 \pm 0.04$	$0.60 \pm 0.30$	$0.11 \pm 0.02$	$0.60 \pm 0.10$

**Figure 2.** (a) AERONET level 1.5 retrieved  $\tau_{440\text{ nm}}$  and (b) AE(440–870 nm) during the ChArMEs 2012 campaign at the five stations (see Table 1 for station descriptions). (c) AERONET version 2 level 1.5 size distributions retrieved for 9, 10, and 11 July. NA indicates no data availability.

of the total coarse mode and the fine mode were retrieved at Barcelona and Athens, whereas the volume concentration profiles of fine, coarse spherical, and coarse spheroid modes were retrieved at Évora, Bucharest, and Granada because of the availability of depolarization information.

At Évora it was clearly observed that the aerosol was located below 1000 m a.s.l., within the planetary boundary layer, and concentrations were very low, ranging from 25 to  $46 \mu\text{m}^3 \text{cm}^{-3}$ . No advected aerosol layers were observed for the analyzed period.

At Granada a clear predominance of coarse spheroid particles reaching altitudes around 6000 m a.s.l. was observed on 9 July, related to the mineral dust event. A small contribution of fine particles was also observed during the 3 days. Values of the volume concentration (below  $50 \mu\text{m}^3 \text{cm}^{-3}$  for the total concentration) indicate a medium intensity dust event, which was considerably decreasing with time. Concentration values around  $30 \mu\text{m}^3 \text{cm}^{-3}$  on 9 July for the coarse spheroid mode went down to values below  $20 \mu\text{m}^3 \text{cm}^{-3}$ . The altitude

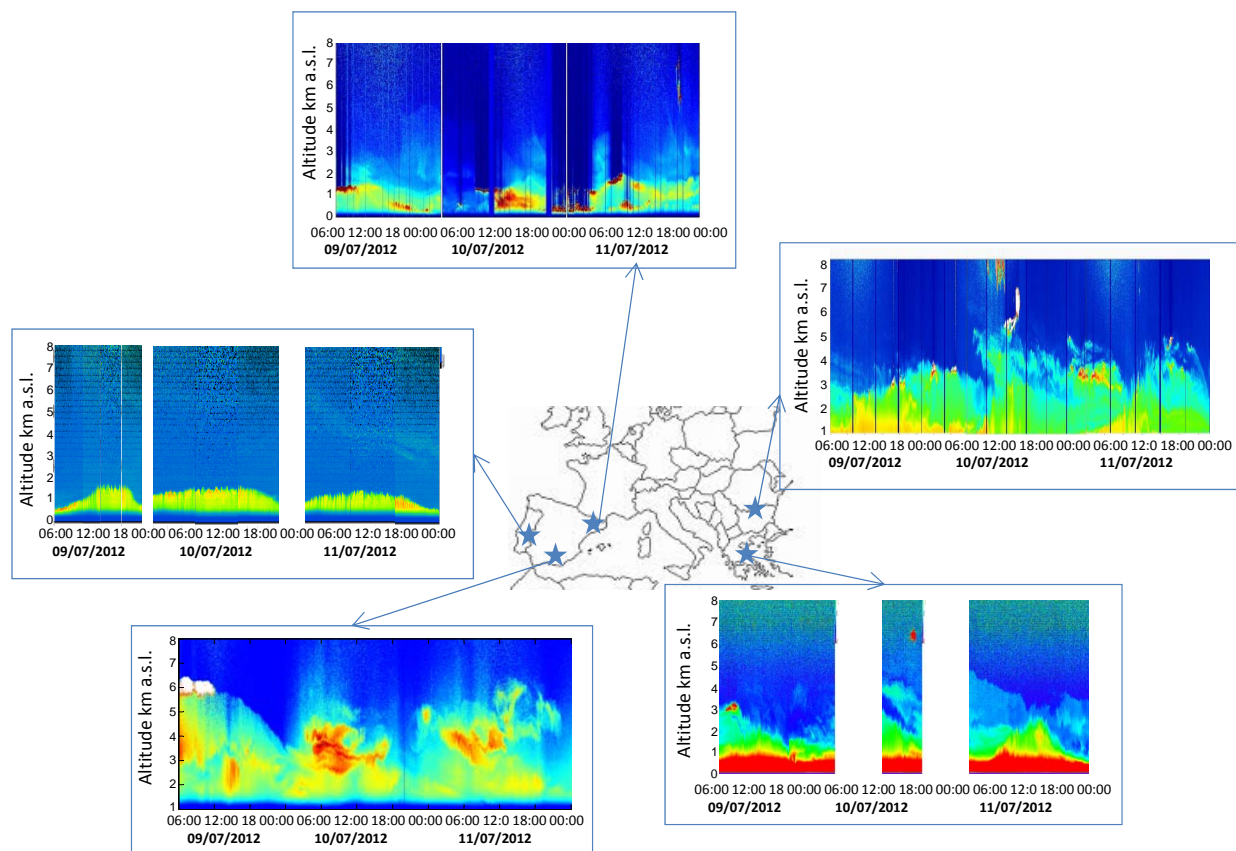


**Figure 3.** RCS at 532 nm (1064 nm at Athens) in arbitrary units for the five stations during the ChArMEx 2012 measurement campaign.

of the mineral dust layers was also decreasing from 6000 to 4000 m a.s.l. for the highest layers.

At the Barcelona site, an aerosol layer dominated by fine particles with a slight presence of coarse particles was observed between 2000 and 4000 m a.s.l. on 11 July, these coarse particles being possibly related to a faint presence of mineral dust. The 5-day backward trajectory analysis performed with the HYSPLIT model (Draxler and Rolph, 2003) (not shown) indicates that air masses arriving at this altitude came from the north of Africa through the Iberian Peninsula. This information, together with previous studies (e.g., Wang et al., 2014), suggests that the mineral dust plume was moving from the north of Africa towards the northeast, being detected at Granada and later on at Barcelona. However, the possibility of these coarse particles being linked to the presence of biomass burning from the eastern Iberian Peninsula (see Fig. 5) cannot be dismissed. Depolarization information would be crucial here to discriminate the origin of the aerosol particles arriving at this height above Barcelona and would provide very valuable information for the aerosol typing at the station.

At the Athens station the aerosol reached up to 5000 m a.s.l. and total concentration values of up to  $55 \mu\text{m}^3 \text{cm}^{-3}$  in the free troposphere. The coarse mode was

located below 2000 m a.s.l., whereas a predominance of fine particles was observed at higher altitudes. The top of the aerosol layer was increasing with time from 3800 to almost 5000 m a.s.l. This temporal evolution of the microphysical properties is coherent with the optical properties shown in Sicard et al. (2015) for the same period. It is worth pointing out that on 11 July, coarse particles were detected between 3000 and 4800 m a.s.l. at this station, probably related to the arrival of mineral dust as indicated by the column-integrated values. Backward trajectory analysis with HYSPLIT (not shown) revealed a change in the trajectory of the air masses arriving at 3500 m a.s.l., coming from northern Africa, which would explain the presence of mineral dust on 11 July. However, according to the trajectories and the different characteristics, the mineral dust observed at Athens corresponds to a different plume than the one observed above Granada and faintly above Barcelona.

At Bucharest, a similar volume concentration of fine and coarse particles was observed on 9 and 10 July, reaching total volume concentration values around  $35 \mu\text{m}^3 \text{cm}^{-3}$ . The observed coarse particles were spherical according to LIRIC; therefore, the presence of mineral dust at this region can be totally neglected. On 11 July a strong increase in the fine mode volume concentration was observed between 2500 and

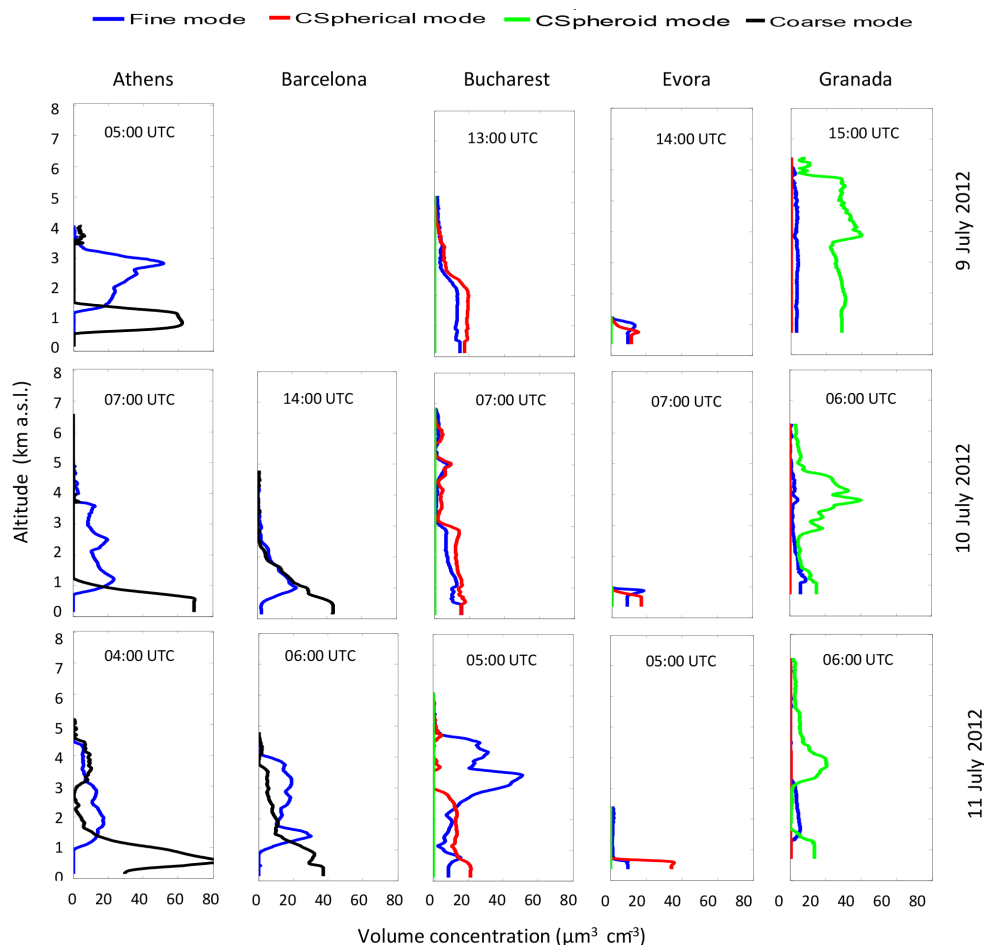


**Figure 4.** Volume concentration profiles of the total coarse mode and the fine mode at Barcelona and Athens, and volume concentration profiles of fine, coarse spherical, and coarse spheroid modes at Évora, Bucharest, and Granada (from left to right) for different periods of 9, 10, and 11 July 2012 (from top to bottom).



**Figure 5.** MODIS FIRMS image indicating the active fires during the five previous days to the 11 July 2012. The red line corresponds to the air-mass 5-day back-trajectory arriving over Bucharest at 3000 m a.s.l. on 11 July 2012.

5000 m a.s.l., with values reaching up to  $55 \mu\text{m}^3 \text{cm}^{-3}$ , suggesting the advection of an aerosol plume dominated by fine particles at this altitude. Again, this is in agreement with the optical properties presented in Sicard et al. (2015), where a larger spectral dependence (related to finer particles) is observed at Bucharest station in the height range between 3 and 4 km a.s.l. As suggested in the study by Sicard et al. (2015), this large spectral dependence of the backscatter coefficient could have originated in the presence of fine particles related to the advection of smoke. The combined information provided by backward trajectory analysis and MODIS FIRMS comes to confirm the presence of active fires along the air mass paths arriving at Bucharest on 11 July (Fig. 5).

The use of the depolarization information as input in LIRIC in the stations of Bucharest, Évora, and Granada provided additional information that is very valuable for aerosol typing. In the cases of Bucharest and Granada, this information turned out to be very useful for the characterization of the aerosol types and their distribution in the vertical coord-

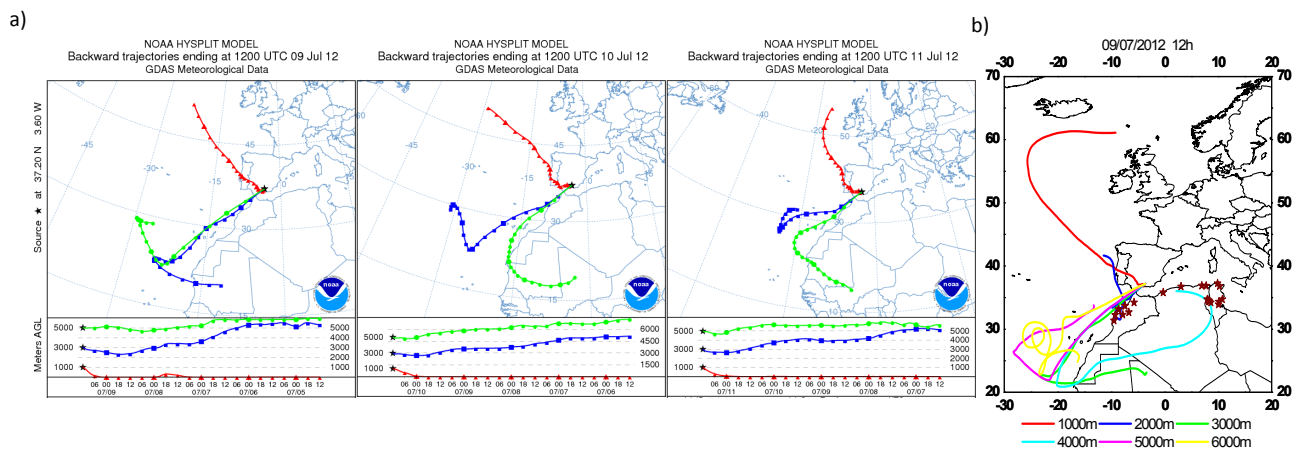


**Figure 6.** (a) Five-day backward trajectories arriving over Granada on 9, 10, and 11 July 2012 at 12:00 UTC (from left to right) computed by the HYSPLIT model. (b) Locations of the main industrial activity in the north of Africa (brown stars) taken from Rodríguez et al. (2011) together with the 5-day backward trajectories arriving at the Granada experimental site on 9 July 2012 at 12:00 UTC.

dinates. The differences in the aerosol type were already evidenced in the columnar volume size distributions retrieved by the AERONET code (Fig. 2), and here LIRIC confirmed that these two stations presented really different situations. The volume concentration profiles retrieved with LIRIC indicated a predominance of the spheroid mode in Granada and a predominance of spherical particles in Bucharest, highlighting very different aerosol composition in the coarse mode. However, at stations such as Barcelona or Athens where lidar depolarization was not measured, ancillary information, e.g., backward trajectories or sun-photometer-derived optical properties, was needed to discriminate whether the coarse mode was related to non-spherical particles, usually associated with mineral dust, or with spherical particles, mostly present in cases of anthropogenic pollution or aged smoke. Therefore, here we have a clear example of the importance and the potential of the depolarization measurements in the vertical characterization of the aerosol particles and for aerosol typing.

#### 4.1.3 Temporal evolution of the aerosol microphysical property profiles

The continuous analysis of the aerosol microphysical properties profiles during the 3 days provided very valuable information about the dynamics of the aerosol layers and revealed LIRIC's potential to retrieve information with a high temporal resolution. Because of the uninterrupted lidar measurements at Granada from 12:00 UTC on 9 July 2012 to 00:00 UTC on 12 July and the frequent AERONET retrievals due to good weather conditions, a more detailed analysis was performed at this station. A total of 60 different LIRIC retrievals were performed based on 60 lidar data sets and 21 AERONET inversion products. The retrieval of microphysical properties was performed using 30 min averaged lidar

data (in order to reduce noise on the lidar profiles) and the closest in time AERONET retrieval, considering only those data with time differences lower than 3 h.

In addition, the Granada station was affected by a mineral dust event during the whole period as already shown in previous sections. This fact is of special interest since the retrieval of the mineral dust microphysical is not so straightforward, and they are not so well characterized. Up to our knowledge not many comprehensive studies on dust microphysical properties vertical profiles have been performed (Tsekeri et al., 2013; Wagner et al., 2013; Granados-Muñoz et al., 2014; Noh, 2014) because of the difficulty of the retrievals due to different factors, e.g., the high temporal variation and non-uniform distribution of dust aerosol concentration around the globe (Sokolik and Toon, 1999; Formenti et al., 2011), mineral dust's highly irregular shape, and the chemical and physical transformations dust suffers during its transport (Sokolik and Toon, 1999; Chen and Penner, 2005; Formenti et al., 2011).

The dust outbreak analyzed here started over the Granada station on 7 July 2012 as indicated by sun-photometer data and the model forecast from previous days (not shown). Thus, it was already well developed when the intensive measurement period started. The 5-day backward trajectories analysis performed with the HYSPLIT model indicated that the air masses arriving at Granada on 9 and 11 July came from Africa, passing by the northern African coast above 2500 m a.s.l. and from the North Atlantic Ocean through the southwestern Iberian Peninsula below this altitude (Fig. 6). On 10 July the air masses came from the central part of the Sahara through the northern African coast for heights above 5000 m a.s.l., from the Atlantic Ocean going along the coast of Africa between 2500 and 5000 m a.s.l., and from the North Atlantic Ocean, overpassing the southwestern Iberian Peninsula below 2500 m a.s.l.

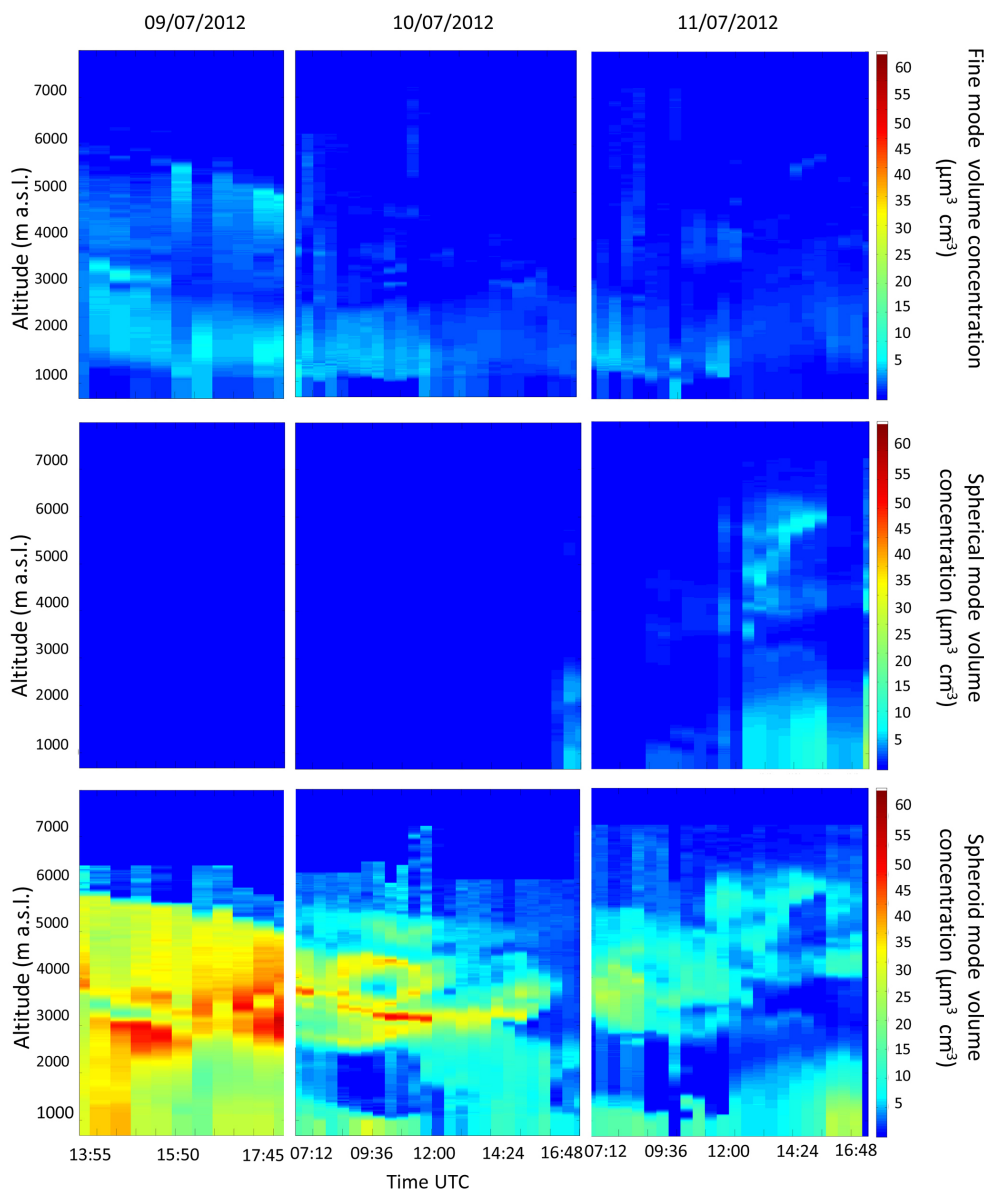


**Figure 7.** Time series of the volume concentration profiles (in  $\mu\text{m}^3 \text{cm}^{-3}$ ) for the fine mode (upper part), coarse spherical mode (middle part), and coarse spheroid mode (lower part) for days 9, 10, and 11 July 2012 (from left to right).

Figure 7 shows the time series of the volume concentration profiles retrieved with LIRIC. It is clearly observed that the dust event was decreasing its intensity along the whole study period, with the largest aerosol concentrations for the coarse spheroid mode retrieved on 9 July ( $\sim 35 \mu\text{m}^3 \text{cm}^{-3}$ ) and the lowest concentrations on 11 July ( $\sim 15 \mu\text{m}^3 \text{cm}^{-3}$ ), in agreement with AERONET data. Maximum values of total volume concentration were around  $60 \mu\text{m}^3 \text{cm}^{-3}$  on 9 July. There was a strong predominance of the coarse spheroid mode during the whole period, with maximum values on 9 July in the afternoon, reaching values of up to  $55 \mu\text{m}^3 \text{cm}^{-3}$ . Some fine particles were also observed, with larger volume concentrations during the first day ( $\sim 10 \mu\text{m}^3 \text{cm}^{-3}$ ). For this first day

of measurements, fine particles reached altitudes of around 6000 m a.s.l., whereas on 10 and 11 July larger volume concentration values were confined to the lowermost region from surface up to 3 km a.s.l. The presence of this fine mode in the upper layers might be related to the advection of anthropogenic pollutants coming from Moroccan industrial activity in the north of Africa mixed with the mineral dust as reported in previous studies (Basart et al., 2009; Rodríguez et al., 2011; Valenzuela et al., 2012, 2014; Lyamani et al., 2015). Figure 6b reveals that air masses overpassed northern African industrial areas before reaching Granada. However, it is also well known that mineral dust emissions produce a submicronic size mode (e.g., Gomes et al., 1990; Alfaro

and Gomes, 2001). Depolarization lidar observations over the Mediterranean have illustrated that irregularly shaped fine dust particles significantly contribute to aerosol extinction over the boundary layer during dust transport events (Mamouri and Ansmann, 2014). A more detailed analysis with additional data (e.g., chemical components measurements, single scattering albedo profiles) would be needed in order to come to a quantitative attribution of soil dust and anthropogenic particles to the fine mode.

The contribution of the fine mode in the lowermost part may be due mainly to anthropogenic sources of local origin. From 11 July around 12:00 UTC up to the end of the study period, an increase in the coarse spherical mode concentration was observed. This increase in the coarse spherical mode was associated with a decrease in the particle linear depolarization profiles  $\delta_{532\text{nm}}^{\text{p}}$  obtained from the lidar data according to Bravo-Aranda et al. (2013) as shown in Fig. 8. On 9 July the values of  $\delta_{532\text{nm}}^{\text{p}}$  were around 0.30 in the layer between 3 and 5 km a.s.l. These values are representative of pure Saharan dust (Freudenthaler et al., 2009). However, they decreased down to 0.25 during the following days, indicating either a possible mixing of dust particles with anthropogenic aerosols or aging processes affecting the mineral dust. During 10 July in the late afternoon and 11 July, a decrease in the fine mode coinciding with an increase in the coarse spherical mode was observed. The simultaneous decrease in the fine mode and increase in the coarse spherical particles together with the decrease in  $\delta_{532\text{nm}}^{\text{p}}$  point to processes such as mineral dust aging and/or aggregation processes. However, additional analysis would be necessary to confirm this hypothesis.

According to  $\delta_{532\text{nm}}^{\text{p}}$  profiles, a mineral dust layer was clearly located above 2500 m a.s.l. or even at higher altitudes depending on the analyzed period (see Fig. 10). Below this altitude, values were lower indicating a mixing of the mineral dust with anthropogenic particles from local origin. In the case of LIRIC, these vertical structures were not so clearly defined, and a more homogeneous structure was detected. Values of the fine and coarse mode volume concentration presented very low variations with height when compared to  $\delta_{532\text{nm}}^{\text{p}}$  profiles. This vertical homogeneity is related to the assumption of height independence of properties such as the refractive index, size distribution of the modes, or the sphericity, which according to the results presented in previous studies (Wagner et al., 2013; Granados-Muñoz et al., 2014), is an issue that needs to be carefully considered in the analysis of the results retrieved with the LIRIC algorithm.

Despite the limitations in the use of LIRIC, the analysis presented here shows that LIRIC can reliably provide microphysical property profiles with high vertical and temporal resolution even in cases of mineral dust. The LIRIC algorithm can be a useful tool to detect changes in the aerosol composition possibly associated with processes affecting the mineral dust particles such as aging or nucleation, even

though additional information is needed for more in-depth analysis.

## 4.2 Evaluation of the mineral dust models

In order to obtain a general overview of the dust horizontal extension, Fig. 9 shows the standard aerosol optical depth product retrieved using the dark-target approach from MODIS/Terra (Remer et al., 2005, and references therein) and the AERUS-GEO from MSG/SEVIRI (Carrer et al., 2014) for the three analyzed days (9–11 July 2012).

Satellite data showed the presence of an aerosol plume extending from the northern African coast towards the east with a higher aerosol load, as  $\tau_{\lambda}$  values from MODIS sensor indicate, mainly affecting the southeast of the Iberian Peninsula and the south of Italy (Fig. 9). As indicated by the data presented in the previous section, this plume corresponds to the mineral dust event, whereas a different plume is observed above the Balkans area. The pathways of the aerosol plumes suggested by satellite data are in agreement with both the meteorological analyses of ECMWF and HYSPLIT air mass trajectories based on GDAS analyzed meteorological fields at 2 km a.g.l. presented in the study by Wang et al. (2014). The air masses were moving from Spain and Portugal to the east, whereas in the Balkans region they were moving southwards.

$\tau_{550\text{nm}}$  data simulated by BSC-DREAM8b, DREAM8-NMME, NMMB/BSC-Dust, and COSMO-MUSCAT are shown in Fig. 10. In general, when comparing to the satellite data in Fig. 9, the aerosol plume located above the Balkans region is not captured by the models. This is not surprising, since it is not composed of mineral dust particles, as indicated by our aerosol volume concentration profiles, shown in the previous section, and suggested in previous studies (e.g., Sicard et al., 2015). The different models correctly forecast the dust plume leaving the north of Africa and moving towards the east and the dust plume reaching Athens, as also indicated by satellite data. However, the decrease in  $\tau_{550\text{nm}}$  values with time observed with satellite data and in LIRIC profiles is not well captured by any of the different models. Regarding the extension of the dust event, in general it is better captured by BSC-DREAM8b and NMMB/BSC-Dust, whereas COSMO-MUSCAT and DREAM8-NMME tend to overestimate the mineral dust horizontal extension when compared to the satellite data.

Focusing on the five stations analyzed in this study, the models showed that the Granada station was affected by the mineral dust outbreak during the whole analyzed period, in agreement with the analyzed data. No presence of mineral dust was forecast above Évora, as expected from the measurements, except for COSMO-MUSCAT, which predicted fair low values of dust  $\tau_{550\text{nm}}$  above the station. BSC-DREAM8b, DREAM8-NMME, and NMMB/BSC-Dust indicated no presence of dust above Barcelona, even though it was located close to the edge according to BSC-DREAM8b.

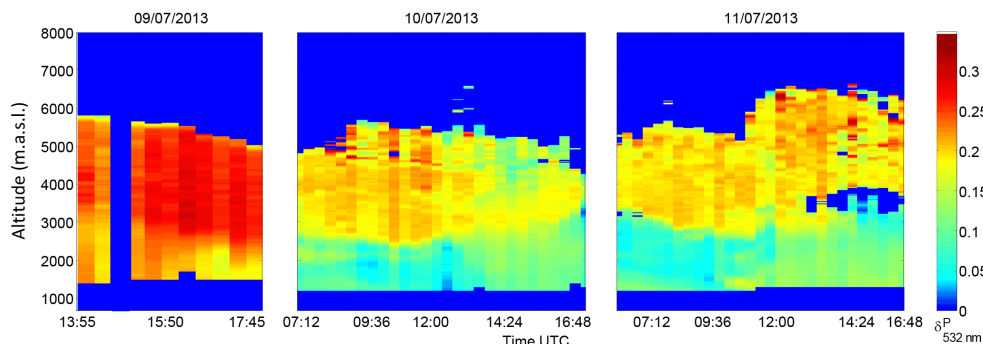


**Figure 8.** Time series of the  $\delta P_{532\text{nm}}^{\text{P}}$  profiles retrieved from the Granada lidar system at different time intervals during the ChArMEx July 2012 intensive measurement period. The dark blue color represents regions and time periods where no data were retrieved.

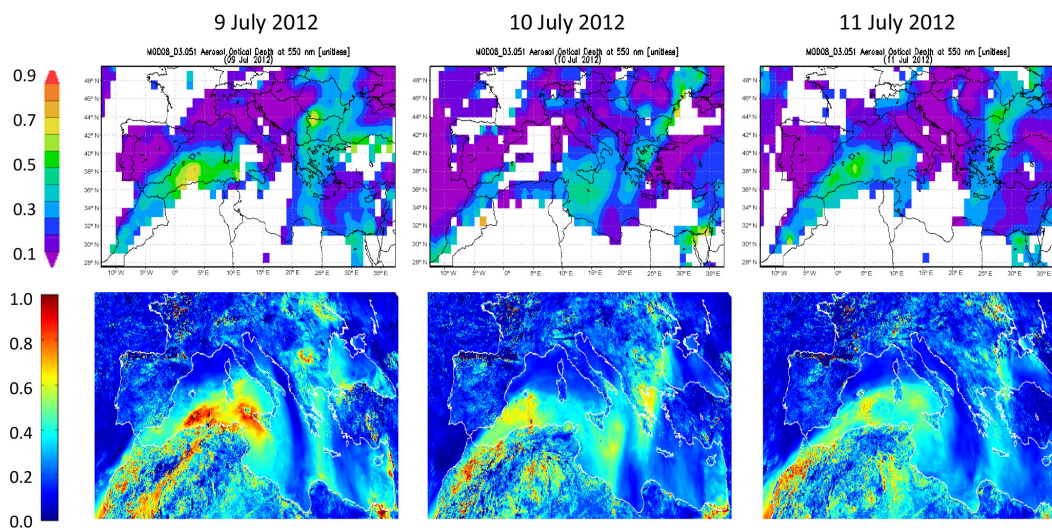


**Figure 9.**  $\tau_{550\text{nm}}$  from MODIS/Terra (top) and  $\tau_{675\text{nm}}$  daytime mean from MSG-SEVIRI (bottom) on 9, 10, and 11 July.

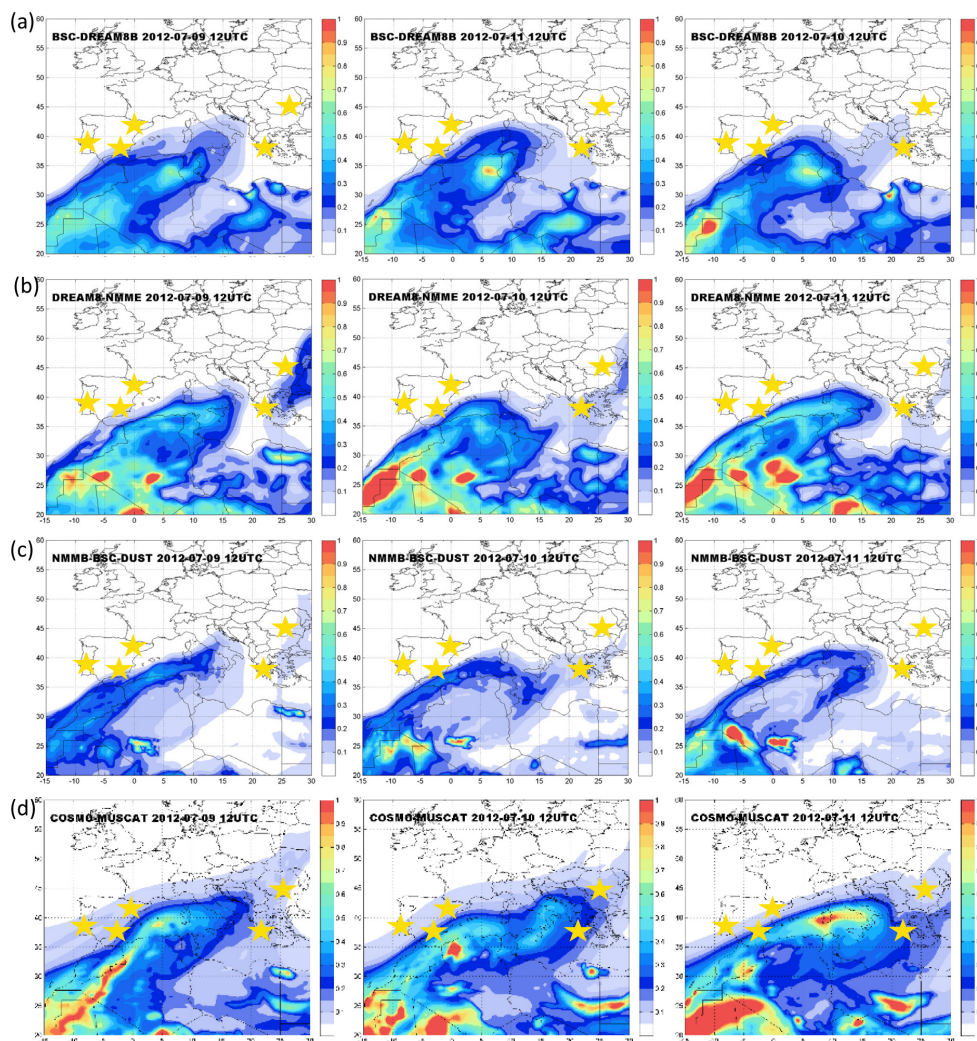
As in the case of Évora, almost negligible values were forecast above the station by COSMO-MUSCAT. This would be in agreement with the previous data except for the possible dust layer observed on 11 July.

In the eastern region, the station of Athens was affected by mineral dust during the 3 days according to the DREAM8-NMME model and COSMO-MUSCAT, only on 10 July according to NMMB/BSC-Dust, and on 10 and 11 July according to BSC-DREAM8b. As indicated by the analysis in the previous section, mineral dust was observed only on 11 July and the models seem to not completely capture the event at Athens. However, in this case the situation is quite more complex than at the western stations. Athens is located at the edge of the mineral dust plume during the 3 analyzed days. Slight changes in the horizontal distribution of the dust related to the model uncertainty and the relatively coarse horizontal resolution may highly influence the results. In the case of Bucharest, BSC-DREAM8b, DREAM8-NMME, and NMMB/BSC-DUST foresaw no influence of the mineral dust. Conversely, COSMO-MUSCAT forecast mineral dust

during the 3 days, with larger loads on 10 and 11 July, overestimating the extension of the mineral dust plumes as previously stated.

Due to the relatively coarse horizontal resolution of the model data presented in Fig. 10 compared to the single-site measurements at the five analyzed stations, it is worth evaluating in more detail the mineral dust mass concentration profiles provided by the models at the specific locations of our interest. To perform this evaluation, mineral dust mass concentration profiles provided by the BSC-DREAM8b, NMMB/BSC-Dust, DREAM8-NMME, and COSMO-MUSCAT models are evaluated against LIRIC results. The main focus is at the Granada station since this site presents a larger number of mineral dust profiles due to the characteristics of the mineral dust event and allows evaluation of the temporal evolution of the dust microphysical properties.

Figure 11 shows the dust mass concentration profiles provided by the four models and LIRIC every 3 h from 9 July at 15:00 to 11 July at 18:00. From the profiles presented in



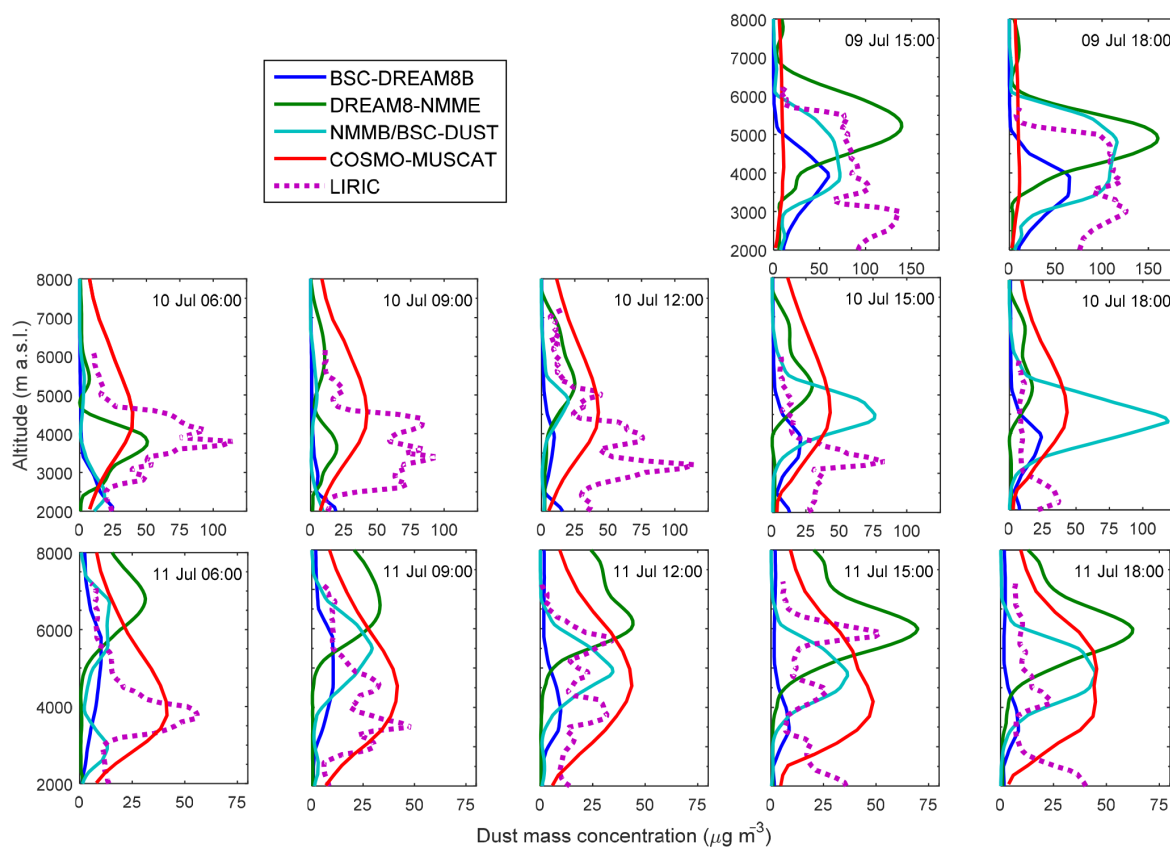
**Figure 10.**  $\tau_{550\text{nm}}$  forecast by the (a) BSC-DREAM8b, (b) DREAM8-NMME, (c) NMMB/BSC-Dust, and (d) COSMO-MUSCAT models for 9, 10, and 11 July 2012 at 12:00 UTC over Europe and northern Africa. The yellow stars represent the location of the stations where microphysical properties profiles are retrieved with LIRIC.

Fig. 11,  $C_m$ , the integrated mass concentration for each profile and the correlation coefficient,  $R$ , between LIRIC and the different models are calculated and presented in Fig. 12. Figure 13 shows the profiles of statistical parameters such as  $R$  obtained for LIRIC and the model time series, RMSE, NMB, and NMSD, calculated as described in Sect. 3 for every altitude level. These three figures need to be analyzed and discussed as a whole in order to cover all aspects of the model performance regarding the temporal and vertical coordinates. An independent interpretation of each of the presented statistical parameters might be misleading at some points and lead to erroneous conclusions.

According to Figs. 11, 12, and 13, BSC-DREAM8b shows a good temporal correlation with LIRIC, providing larger values on 9 July than on 10 and 11 July, as observed in the experimental data. The correlation coefficient  $R$  between BSC-

DREAM8b and LIRIC time series is larger than 0.5 for most of the altitudes (Fig. 13a). However, the model strongly underestimates the aerosol load during the 3 studied days, as indicated by the NMB in Fig. 13c. Positive and larger than 0.5 values of  $R$  and the small difference between LIRIC and BSC-DREAM8b values of  $C_m$  during most of the analyzed period in Fig. 12 indicate that BSC-DREAM8b provides a good estimation of the mineral dust vertical distribution.

A relatively good performance of DREAM8-NMME is observed up to 10 July at 06:00 UTC, when  $\tau_{440\text{nm}}$  was larger than 0.2. During this period the model captured quite well the maximum values and the aerosol load as observed in Fig. 11 and indicated by the integrated mass concentration values in Fig. 12, close to those obtained with LIRIC. Despite this good performance during the first part of the analyzed period, NMB values in Fig. 13c suggest an overall un-



**Figure 11.** Dust mass concentration profiles obtained with LIRIC (dotted line) and BSC-DREAM8b-v2, DREAM8-NMME, DREAMABOL, and NMMB/BSC-Dust for Granada station every 3 h on 9, 10, and 11 July 2012.

derestimation of the aerosol load below 5000 m a.s.l., where it is higher, and overestimation above 5000 m a.s.l., where concentration values are lower according to LIRIC. From 3500 m a.s.l., good temporal correlation is observed between LIRIC and DREAM8-NMME, but  $R$  goes close to 0 below this altitude (Fig. 13a). Regarding the vertical distribution of the load,  $C_m$  values in Fig. 12 present very small differences with LIRIC before 10 July at 06:00, but this difference increased afterwards. Absolute values of  $R$  in Fig. 12 are usually larger than 0.5 and larger than those retrieved for the other models, indicating good correlation. However, they oscillate from negative to positive values, indicating a vertical shift in the location of the dust layers during some of the analyzed periods.

NMMB/BSC-Dust shows a better performance on 9 July, with  $\tau_{440\text{nm}}$  values around 0.3, especially in the layer between 2500 and 6000 m a.s.l. The difference between LIRIC and the model-integrated mass concentration is also lower during 9 July. However, in general the model tends to underestimate the aerosol load below 4.5 km a.s.l. (Fig. 13c). Overestimation of the mass concentration is observed above this altitude though. NMMB/BSC-Dust correctly follows the aerosol load decrease with time as indicated by positive correlation values in Fig. 13a, but it presents a lower tempo-

ral correlation compared to the other models (except for COSMO-MUSCAT). Values of  $C_m$  in Fig. 12 are close to those of LIRIC, indicating that it correctly forecast the location of the aerosol load. Nonetheless, low values of  $R$  indicate that the vertical distribution of the aerosol layers needs to be improved. For this model it is worth pointing out the unrealistic increasing maximum at 5000 m a.s.l. at 15:00 and 18:00 on 10 July (Fig. 11). However, this maximum is very similar to the one provided by LIRIC between 06:00 and 12:00 UTC. Therefore, it could be due to a time shift of the model when compared to the LIRIC values. To check this hypothesis, the correlation between LIRIC and the models considering a 3 h delay is calculated (Supplement Fig. S5). Correlation between LIRIC and NMMB/BSC-Dust for simultaneous data is on average below 0.5 (Fig. 13a), indicating that the model does not reproduce very well the temporal evolution of the dust profiles. This correlation slightly increases between 3500 and 4500 m a.s.l. when considering a 3 h delay between LIRIC and the model, but decreases at the other altitudes. Therefore, it does not appear to be a systematic delay between the model and LIRIC profiles. However, in the future it will be beneficial for the modeling community to gather a more extended database of continuous lidar measurements with similar characteristics to the one presented

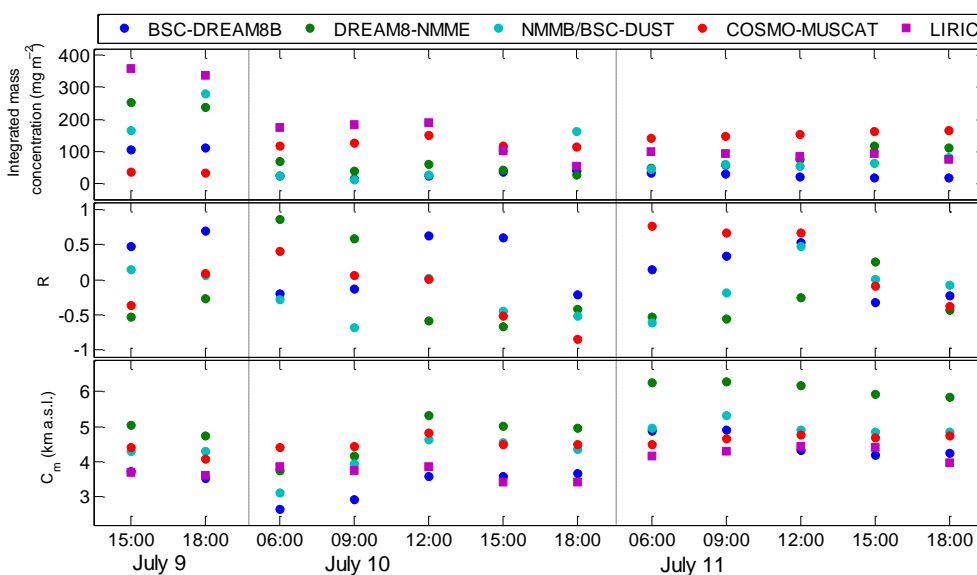


**Figure 12.** (From top to bottom) Time series of the integrated mass concentration values (above 2 km in altitude) retrieved from LIRIC and the four evaluated model vertical profiles for the period between 15:00 UTC on 9 July 2012 and 18:00 UTC on 11 July 2012. Time series of the correlation coefficient  $R$ , between LIRIC-derived mass concentration profiles, and each one of the four evaluated models for the same period. Time series of the dust center of mass,  $C_m$ , obtained from LIRIC and the model profiles.

here in order to further explore and improve the possible existence of delays between the model forecast and experimental data.

COSMO-MUSCAT shows an increase in the mineral dust load during the analyzed period, with an increasing maximum approximately located between 4 and 5 km. This behavior is totally opposite to the one observed in LIRIC profiles that shows a decrease in the volume concentration with time, as indicated by the negative values of  $R$  in Fig. 13a. According to the integrated mass concentration values in Fig. 12, COSMO-MUSCAT underestimates the dust load during the first half of the analyzed period, whereas an overestimation of the dust load occurs in the second half. These two opposite behaviors seem to cancel and, as a result, NMB values in Fig. 13c are closer to zero below 4 km than for the other models, leading to erroneous conclusions. The locations of  $C_m$  and  $R$  values in Fig. 12 indicate a good performance of the model regarding vertical distribution on 9 and 11 July and the afternoon of 10 July. Again, negative  $R$  values indicate a vertical shift in the location of the maximum concentration values during some periods, as also observed in Fig. 11.

The four models have been shown to have advantages and disadvantages, but a clear superior performance of any of the four has not been observed. As a general result, the four models tend to underestimate LIRIC values during the whole period, except for COSMO-MUSCAT, which clearly overestimates the dust mass concentration from the afternoon of 10 July onwards. DREAM8-NMME and NMMB/BSC-Dust show a better performance, both regarding the dust load and

the temporal evolution of the event when the aerosol load observed with the ground-based instrumentation is higher. The temporal evolution of the event is mostly followed by the BSC models (namely the BSC-DREAM8b, DREAM8-NMME, and NMMB/BSC-Dust models) as indicated by the positive correlation with LIRIC time series, whereas COSMO-MUSCAT shows an opposite behavior (Fig. 13a). BSC-DREAM8b shows the minimum values of the RMSE below 4 km, where most of the aerosol load is located, and maximum values are obtained for DREAM8-NMME. However, no statistically significant difference between the models is clearly observed. BSC-DREAM8b, DREAM8-NMME, and COSMO-MUSCAT are not able to capture the high temporal variability observed with LIRIC, as indicated by the large absolute values of NMSD in Fig. 13d. They range between  $-0.5$  and  $-1$  below 6 km a.s.l. for COSMO-MUSCAT and BSC-DREAM8b and between  $-1$  at the lower altitudes and 2 at the upper levels for DREAM8-NMME. NMMB/BSC-Dust shows a good performance in this case, with values close to 0 from 3 km upwards.

The location of  $C_m$ , which is an indicator of the vertical distribution of the dust mass concentration, is similar in the case of LIRIC and the models (Fig. 12). Despite the models being capable of reproducing the temporal evolution of  $C_m$ , in general they tended to locate the dust load at higher altitudes, as indicated by the larger values of  $C_m$  obtained. Discrepancies are especially relevant in the case of DREAM8-NMME after 10 July in the afternoon. During this event, the BSC-DREAM8b model presented the lowest differences with LIRIC regarding  $C_m$  height. COSMO-

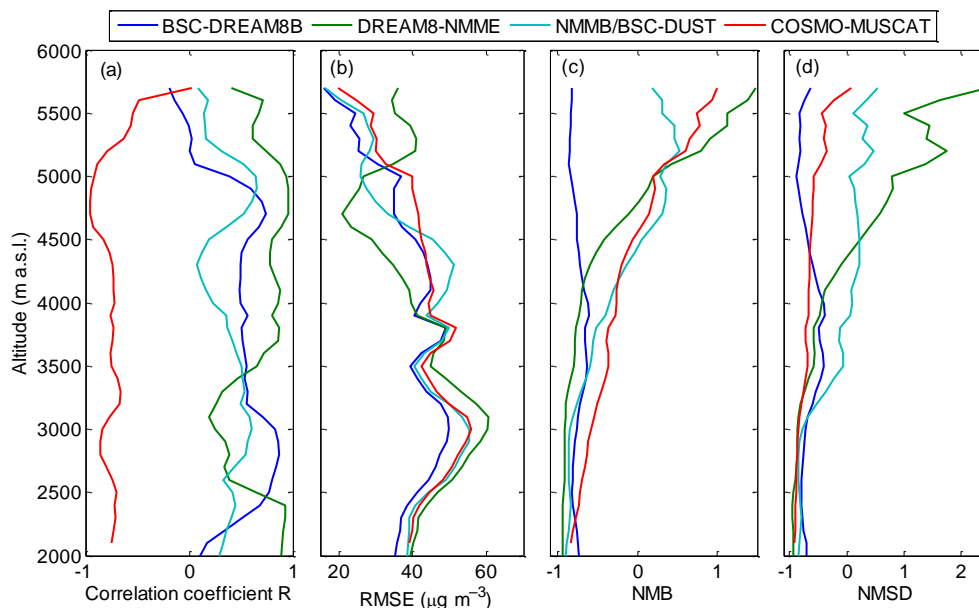


**Figure 13.** Vertical profiles of the correlation coefficient between LIRIC and the model time series for every altitude level, the root mean square error RMSE, the normalized mean bias NMB, and the normalized mean standard deviation NMSD.

MUSCAT and NMMB/BSC-Dust presented the lower discrepancies on 11 July. These results are comparable to those in the study by Biniotoglou et al. (2015).

Even though they forecast the  $C_m$  fairly well, the analyzed models provided much smoother profiles than the ones retrieved with LIRIC, with usually a single-broad maximum located at different altitudes depending on the model. This result is not surprising due to the coarser vertical resolution of the models compared to lidar profiles, which can provide more detailed information about the vertical structures of mineral dust. The vertical correlation between the models, shown in Fig. 12b, oscillates between positive and negative values, indicating a shift in the location of the maximum peaks in those cases when it is negative.  $R$  values range between 0.01 and 0.85 in absolute value. The correlation obtained in the present analysis is lower than the ones presented in Biniotoglou et al. (2015), where most of the data presented determination coefficient ( $R^2$ ) values above 0.5. This is related to the fact that in the study by Biniotoglou et al. (2015) selected mineral dust events with higher aerosol loads ( $\tau_{440} > 0.15$ ) were presented, whereas in this study the continuous evolution of the dust event was analyzed with  $\tau_{440}$  ranging between 0.07 and 0.40. Therefore, according to the present study models seem to show a better performance in cases of higher aerosol load.

Model profiles were also obtained at the stations of Athens, Barcelona, Bucharest, and Évora in order to evaluate their performance at stations where there is a slight or no presence of mineral dust. At Athens (Fig. S1 in the Supplement) almost negligible mass concentration values were forecast by the different models, with the exception

of DREAM8-NMME. This model indicated the presence of mineral dust in mass concentrations up to  $100 \mu\text{g m}^{-3}$ , reaching 4000 m a.s.l. on 10 July and up to  $65 \mu\text{g m}^{-3}$  on 11 July, which is not in agreement with LIRIC results. In spite of the disagreement, it is worth pointing out that the dust layer observed at Athens between 3000 and 5000 m a.s.l. on 11 July according to LIRIC data was correctly forecast by the different models. At the Barcelona station (Fig. S2), DREAM8-NMME was not in agreement with the experimental results since it forecast dust mass concentrations of up to  $100 \mu\text{g m}^{-3}$  and located below 2000 m a.s.l. At Bucharest (Fig. S3), large dust concentrations were forecast between 3000 and 7000 m a.s.l. by BSC-DREAM8b, DREAM8-NMME, and NMMB/BSC-Dust on 9 July. On 10 and 11 July the dust load forecast by the models was much lower, even though it reached up to  $50 \mu\text{g m}^{-3}$ . This is not in agreement with our experimental results since only coarse spherical and fine particles and no mineral dust should be forecast here. Finally, at the Évora station (Fig. S4), DREAM8-NMME forecast dust mass concentration lower than  $10 \mu\text{g m}^{-3}$  below 2000 m a.s.l. COSMO-MUSCAT forecast similar concentrations above 2000 m a.s.l. These mass concentration values are almost negligible and therefore good agreement can be considered. In general, good results were provided by the different models at the five stations. However, DREAM8-NMME seems to be overestimating the dust mass concentrations at those stations affected by aerosol types different to mineral dust.

An in-depth analysis of the causes of the discrepancies between the models and LIRIC is beyond the scope of this study, especially taking into account that they showed a sim-

ilar performance here, with none of them proving to be more accurate than the others. In general we observed that the BSC models showed a similar behavior between them. Differences were clearly observed when they were compared to COSMO-MUSCAT, based on a different philosophy. However, none of them showed a statistically significant better performance. Differences between the obtained results lie in the different approaches used in the different models, the different meteorological fields used, dust sources, horizontal and vertical transport schemes, different resolutions, etc., as already pointed out in Binietoglou et al. (2015). Robust conclusions in this respect cannot be drawn from this study and would require wider databases with higher temporal and spatial coverage in order to cover the different aspects of the model calculations, and more dedicated studies. Nonetheless, the comparison presented here provided valuable results since it addresses the points of discrepancy and proves LIRIC's potential as a tool for future model evaluations. Information inferred from the results obtained here could be used for the planning of future validation strategies and campaign management.

## 5 Summary and conclusions

In this study, the characterization of aerosol microphysical properties at different stations throughout Europe was performed in the framework of the ChArMEx/EMEP 2012 field campaign, in support of which EARLINET lidar stations performed continuous measurements during 72 h. LIRIC profiles were obtained at five different stations in Europe (i.e., Athens, Barcelona, Bucharest, Évora, and Granada) in order to characterize atmospheric aerosol particles both in the vertical and horizontal coordinates and also their temporal evolution during this period. From the analysis of the aerosol microphysical properties at the different stations, two different aerosol plumes were clearly observed: one affecting the western Mediterranean region, loaded with mineral dust, and another one over the Balkans area, mainly composed of fine particles and coarse spherical particles. The Granada station was clearly affected by the mineral dust outbreak during these 72 h, whereas mainly aerosol of local origin affected Évora and Barcelona. The dust plume was also observed above Barcelona on 11 July. A mixture of fine and coarse spherical particles was observed over Bucharest, likely related to the presence of smoke from European fires, whereas at Athens mainly fine particles were observed, except on 11 July, when mineral dust of a different origin from the one in Granada and Barcelona was observed at 3.5 km a.s.l., as indicated by the backward trajectory analysis.

A thorough evaluation of the temporal evolution and the aerosol layer dynamics was possible at the Granada station, where a total of 60 lidar profiles every 30 min and 21 AERONET inversion retrievals were available. The analysis of the microphysical properties profiles retrieved with

LIRIC indicated that the dust event was decreasing in intensity, with larger concentrations on 9 July ( $\sim 35 \mu\text{m}^3 \text{cm}^{-3}$ ) decreasing towards 11 July ( $\sim 15 \mu\text{m}^3 \text{cm}^{-3}$ ), in agreement with AERONET and satellite data. On 9 July there was a strong predominance of the coarse spheroid mode with maximum values in the afternoon, while an increase in the concentration of the coarse spheroid mode up to  $15 \mu\text{m}^3 \text{cm}^{-3}$  was observed during the afternoon of 11 July. This temporal evolution of the microphysical properties reveals possible aging processes of the mineral dust above the station or even mixing processes with different aerosol types.

These results provide a good overview of the aerosol microphysical properties in the Mediterranean region during the ChArMEx campaign. They also highlight the importance of having combined regular AERONET/EARLINET measurements for the characterization of aerosol microphysical properties in the vertical, horizontal, and spatial coordinates with high resolution by means of algorithms such as LIRIC and suggest the importance of extending this kind of measurement. Our study remarks on the capability of LIRIC to be implemented in a simple, automated, and robust way within a network such as EARLINET and during special measurement campaigns obtaining reliable results. In addition, the advantages of the use of depolarization measurements with lidar systems are also emphasized here, since the stations with depolarization capabilities (namely Bucharest, Évora, and Granada) provided much more complete information about the microphysical properties profiles.

The availability of LIRIC output profiles at the five different stations provided regional coverage and made possible a comparison with the modeled dust fields provided by BSC-DREAM8b, NMMB/BSC-Dust, DREAM8-NMME, and COSMO-MUSCAT. The regional comparison revealed quite good agreement with the horizontal distribution of the dust plume forecast by the BSC models (based on a similar philosophy), but lower agreement for COSMO-MUSCAT over the Balkans region.

A more detailed comparison using dust mass concentration profiles derived every 3 h from 06:00 to 18:00 UTC over the 3 days of interest was also performed. The four models tended to underestimate the dust mass concentration when compared to LIRIC results, except for COSMO-MUSCAT on the afternoon of 10 July and on 11 July, which overestimated it. The overall underestimation of the dust mass concentration was between 80 and 100 % for altitudes below 4 km, depending on the model. Above this altitude, DREAM8-NMME and NMMB/BSC-Dust tended to overestimate the dust mass concentration values, reaching up to 150 % overestimation. The agreement between LIRIC and the models was better when determining the vertical location of the mineral dust load, even though the models tended to locate the mineral dust at higher altitudes than seen by lidar, as indicated by the correlation coefficient values and the center of mass location. The correlation coefficient between LIRIC and the models reached absolute values of up to 0.85,

even though in most of the cases the maximum peaks were shifted when compared to LIRIC, showing anticorrelation. The difference in the center of mass location was below 1 km in 65 % of the cases.

A comparison between LIRIC and the models was also performed at the stations of Évora, Barcelona, Athens, and Bucharest. In general, good agreement was obtained for BSC-DREAM8b, NMMB/BSC-Dust, and COSMO-MUSCAT, when no dust is observed. DREAM8-NMME indicated the presence of mineral dust in large concentrations in Athens, Barcelona, and Évora, opposite to LIRIC results, which indicated almost negligible or no presence of mineral dust. BSC-DREAM8b, NMMB/BSC-Dust, and DREAM8-NMME forecast the presence of mineral dust in the vertical coordinate in the Bucharest station, where LIRIC indicated the presence of a different aerosol type (mostly fine and spherical particles), suggesting that the COSMO-MUSCAT philosophy is more adequate for this specific case and location.

The four analyzed models present advantages and disadvantages, but none of them showed a statistically significant better performance when evaluated against LIRIC results. In general, the three BSC models showed more similar results compared against COSMO-MUSCAT, based on a different philosophy, but further conclusions regarding the differences between the models cannot be drawn from our study. A more detailed analysis based on a wider and more specific database designed to cover the different aspects of the model calculations would be required. Results presented here are valuable since they prove LIRIC's potential as a tool for model evaluation and provide valuable information for the planning of future validation strategies and campaign management.

## 6 Data availability

BSC-DREAM8b data and additional information about the model are available at <http://www.bsc.es/projects/earthscience/BSC-DREAM/>.

**The Supplement related to this article is available online at doi:10.5194/acp-16-7043-2016-supplement.**

*Acknowledgements.* This work was supported by the Andalusia Regional Government through projects P12-RNM-2409 and P10-RNM-6299, by the Spanish Ministry of Economy and Competitiveness through projects TEC2012-34575, TEC2015-63832-P, CGL2013-45410-R, CGL2011-13580-E/CLI, CGL2011-16124-E, and CGL2013-46736-R; by the Spanish Ministry of Science and Innovation (project UNPC10-4E-442); the EU through the H2020 project ACTRIS2 (contract number 654109); by the University of Granada through the contract “Plan Propio. Programa 9. Convocatoria 2013”; and by the Department of Economy and Knowledge

of the Catalan autonomous government (grant 2014 SGR 583). M. J. Granados-Muñoz was funded under grant AP2009-0552 from the Spanish Ministry of Education and Science. S. N. Pereira was funded under fellowship SFRH/BPD/81132/2011 and projects FCOMP-01-0124-FEDER-029212 (PTDC/GEO-MET/4222/2012 from the Portuguese Government). S. Basart and J. M. Baldasano acknowledge the CICYT project (CGL2010-19652 and CGL2013-46736) and Severo Ochoa Programme (SEV-2011-00067) of the Spanish Government. BSC-DREAM8b and NMMB/BSC-Dust simulations were performed on the Mare Nostrum supercomputer hosted by Barcelona Supercomputing Center-Centro Nacional de Supercomputación (BSC-CNS). This paper was realized also as a part of the project III43007 financed by the Ministry of Education and Science of the Republic of Serbia within the framework of integrated and interdisciplinary research for the period 2011–2015. It has also received funding from the European Union's Seventh Framework Programme for research, technological development, and demonstration under grant agreement no. 289923 – ITaRS. The CIMEL calibration was performed at the AERONET-EUROPE calibration center, supported by ACTRIS-2 (EUH2020 grant agreement no. 654109). The authors express gratitude to the NOAA Air Resources Laboratory for the HYSPLIT transport and dispersion model; the ICARE Data and Services Center the MODIS team; and the ChArMEx project of the MISTRALS (Mediterranean Integrated Studies at Regional And Local Scales; <http://www.mistrals-home.org>) multidisciplinary research programme.

Edited by: X. Querol

## References

- Alfaro, S. and Gomes, L.: Modeling mineral aerosol production by wind erosion: intensities and aerosol size distribution in source areas, *J. Geophys. Res.*, 106, 18075–18084, doi:10.1029/2000JD900339, 2001.
- Andreae, M.: Biomass burning: Its history, use, and distribution and its impact on environmental quality and global climate, in: *Global Biomass Burning- Atmospheric, Climatic, and Biospheric Implications*, edited by: Levine, J. S., MIT Press, Cambridge, MA, 3–21, 1991.
- Baldauf, M., Seifert, A., Förstner, J., Majewski, D., Raschendorfer, M., and Reinhardt, T.: Operational convective-scale numerical weather prediction with the COSMO model: description and sensitivities, *Mon. Weather Rev.*, 139, 3887–3905, 2011.
- Basart, S., Pérez, C., Cuevas, E., Baldasano, J. M., and Gobbi, G. P.: Aerosol characterization in Northern Africa, Northeastern Atlantic, Mediterranean Basin and Middle East from direct-sun AERONET observations, *Atmos. Chem. Phys.*, 9, 8265–8282, doi:10.5194/acp-9-8265-2009, 2009.
- Basart, S., Pérez, C., Nickovic, S., Cuevas, E., and Baldasano, J. M.: Development and evaluation of the BSC-DREAM8B dust regional model over Northern Africa, the Mediterranean and the Middle East, *Tellus B*, 64, 18539, doi:10.3402/tellusb.v64i0.18539, 2012.
- Biniotoglou, I., Basart, S., Alados-Arboledas, L., Amiridis, V., Argyrouli, A., Baars, H., Baldasano, J. M., Balis, D., Belegante, L., Bravo-Aranda, J. A., Burlizzi, P., Carrasco, V., Chaikovskiy,

- A., Comerón, A., D'Amico, G., Filioglou, M., Granados-Muñoz, M. J., Guerrero-Rascado, J. L., Ilic, L., Kokkalis, P., Maurizi, A., Mona, L., Monti, F., Muñoz-Porcar, C., Nicolae, D., Papayannis, A., Pappalardo, G., Pejanovic, G., Pereira, S. N., Perrone, M. R., Pietruczuk, A., Posyniak, M., Rocadenbosch, F., Rodríguez-Gómez, A., Sicard, M., Siomos, N., Szkop, A., Terradellas, E., Tsekeri, A., Vukovic, A., Wandinger, U., and Wagner, J.: A methodology for investigating dust model performance using synergistic EARLINET/AERONET dust concentration retrievals, *Atmos. Meas. Tech.*, 8, 3577–3600, doi:10.5194/amt-8-3577-2015, 2015.
- Bravo-Aranda, J. A., Navas-Guzmán, F., Guerrero-Rascado, J. L., Pérez-Ramírez, D., Granados-Muñoz, M. J., and Alados-Arboledas, L.: Analysis of lidar depolarization calibration procedure and application to the atmospheric aerosol characterization, *Int. J. Remote Sens.*, 34, 3543–3560, doi:10.1080/01431161.2012.716546, 2013.
- Bösenberg, J., Ansmann, A., Baldasano, J. M., Calpini, B., Chaikovskiy, A., Flamant, P., Mitev, V., Flamant, A., Hågård, A., Mitev, V., Papayannis, A., Pelon, J., Resendes, D., Schneider, J., Spinelli, N., Trickl, T., Vaughan, G., Visconti, G., and Wiegner, M.: EARLINET: a European aerosol research lidar network, in: *Advances in Laser Remote Sensing*, edited by: Dabas, A., Loth, C., and Pelon, J., Ecole Polytechnique, Palaiseau Cedex, France, 155–158, 2001.
- Bréon, F.-M.: How do aerosols affect cloudiness and climate?, *Science*, 313, 623–624, doi:10.1126/science.1131668, 2006.
- BSC-CNS: BSC-DREAM8b v2.0 Atmospheric Dust Forecast System, available at: <http://www.bsc.es/projects/earthscience/BSC-DREAM/>, last access: 2 June 2016.
- Carrer, D., Ceamanos, X., Six, B., and Roujean J.-L.: AERUS-GEO: A newly available satellite-derived aerosol optical depth product over Europe and Africa, *Geophys. Res. Lett.*, 41, 7731–7738, doi:10.1002/2014GL061707, 2014.
- Claquin, T., Schulz, M., Balkanski, Y., and Boucher, O.: Uncertainties in assessing radiative forcing by mineral dust, *Tellus B*, 50, 491–505, doi:10.3402/tellusb.v50i5.16233, 1998.
- Chaikovskiy, A., Dubovik, O., Goloub, P., Balashevich, N., Lopatsin, A., Karol, Y., Denisov, S., and Lapyonok, T.: Software package for the retrieval of aerosol microphysical properties in the vertical column using combined lidar/photometer data (test version), Technical Report, Minsk, Belarus, Institute of Physics, National Academy of Sciences of Belarus, 2008.
- Chaikovskiy, A., Dubovik, O., Goloub, P., Tanré, D., Pappalardo, G., Wandinger, U., Chaikovskaya, L., Denisov, S., Grudo, Y., Lopatsin, A., Karol, Y., Lapyonok, T., Korol, M., Osipenko, F., Savitski, D., Slesar, A., Apituley, A., Arboledas, L. A., Biniotoglou, I., Kokkalis, P., Granados Muñoz, M. J., Papayannis, A., Perrone, M. R., Pietruczuk, A., Pisani, G., Rocadenbosch, F., Sicard, M., De Tomasi, F., Wagner, J., and Wang, X.: Algorithm and software for the retrieval of vertical aerosol properties using combined lidar/radiometer data: Dissemination in EARLINET, 26th International Laser and Radar Conference, Porto Heli, Greece, 2012.
- Chaikovskiy, A., Dubovik, O., Holben, B., Bril, A., Goloub, P., Tanré, D., Pappalardo, G., Wandinger, U., Chaikovskaya, L., Denisov, S., Grudo, J., Lopatin, A., Karol, Y., Lapyonok, T., Amiridis, V., Ansmann, A., Apituley, A., Alados-Arboledas, L., Biniotoglou, I., Boselli, A., D'Amico, G., Freudenthaler, V., Giles, D., Granados-Muñoz, M. J., Kokkalis, P., Nicolae, D., Oschepkov, S., Papayannis, A., Perrone, M. R., Pietruczuk, A., Rocadenbosch, F., Sicard, M., Slutsker, I., Talianu, C., De Tomasi, F., Tsekeri, A., Wagner, J., and Wang, X.: Lidar-Radiometer Inversion Code (LIRIC) for the retrieval of vertical aerosol properties from combined lidar/radiometer data: development and distribution in EARLINET, *Atmos. Meas. Tech.*, 9, 1181–1205, doi:10.5194/amt-9-1181-2016, 2016.
- Chen, Y. and Penner, J. E.: Uncertainty analysis for estimates of the first indirect aerosol effect, *Atmos. Chem. Phys.*, 5, 2935–2948, doi:10.5194/acp-5-2935-2005, 2005.
- Choobari, O. A., Zawar-Reza, P., and Sturman, A.: The global distribution of mineral dust and its impacts on the climate system: A review, *Atmos. Res.*, 138, 152–165, 2014.
- D'Amico, G., Amodeo, A., Baars, H., Biniotoglou, I., Freudenthaler, V., Mattis, I., Wandinger, U., and Pappalardo, G.: EARLINET Single Calculus Chain – overview on methodology and strategy, *Atmos. Meas. Tech.*, 8, 4891–4916, doi:10.5194/amt-8-4891-2015, 2015.
- Draxler, R. R. and Rolph, G. D.: HYSPLIT (HYbrid Single-Particle Lagrangian Integrated Trajectory) model access via NOAA ARL READY website, available at: <http://www.arl.noaa.gov/ready/hysplit4.html> (last access: 25 May 2016), NOAA Air Resources Laboratory, Silver Spring, Md, 2003.
- Dubovik, O. and King, M. D.: A flexible inversion algorithm for retrieval of aerosol optical properties from Sun and sky radiance measurements, *J. Geophys. Res.*, 105, 20673–20696, doi:10.1029/2000JD900282, 2000.
- Dubovik, O., Sinyuk, A., Lapyonok, T., Holben, B. N., Mishchenko, M., Yang, P., Eck, T. F., Volten, H., Muñoz, O., and Veihelmann, B.: Application of spheroid models to account for aerosol particle nonsphericity in remote sensing of desert dust, *J. Geophys. Res.*, 111, D11208, doi:10.1029/2005JD006619, 2006.
- Dulac, F.: An overview of the Chemistry-Aerosol Mediterranean Experiment (ChArMEx), *Geophys. Res. Abstr.*, EGU2014-11441, EGU General Assembly 2014, Vienna, Austria, 2014.
- Eck, T. F., Holben, B. N., Reid, J. S., Dubovik, O., Smirnov, A., O'Neill, N. T., Slutsker, I., and Kinne, S.: Wavelength dependence of the optical depth of biomass burning, urban, and desert dust aerosols, *J. Geophys. Res.*, 104, 31333–31349, doi:10.1029/1999JD900923, 1999.
- Espen Yttri, K., Aas, W., Tørseth, K., Kristiansen, N. I., Lund Myhre, C., Tsyro, S., Simpson, D., Bergström, R., Marečková, K., Wankmüller, R., Klimont, Z., Amman, M., Kouvarakis, G. N., Laj, P., Pappalardo, G., and Prévôt, A.: EMEP Co-operative Programme for Monitoring and Evaluation of the Long-Range Transmission of Air Pollutants in Europe; Transboundary particulate matter in Europe Status report 2012, available at: <http://www.actris.net/Portals/97/documentation/dissemination/other/emep4-2012.pdf> (last access: 9 December 2014), 2012.
- Estellés, V., Utrillas, M. P., Martínez-Lozano, J. A., Alcántara, A., Alados-Arboledas, L., Olmo, F. J., Lorente, J., de Cabo, X., Cachorro, V., Horvath, H., Labajo, A., Sorribas, M., Díaz, J. P., Díaz, A. M., Silva, A. M., Elías, T., Pujadas, M., Rodrigues, J. A., Cañada, J., and García, Y.: Intercomparison of spectroradiometers and Sun photometers for the determination of the aerosol optical depth during the VELETA-2002 field campaign, *J. Geophys. Res.*, 111, D17207, doi:10.1029/2005JD006047, 2006.

- Formenti, P., Schütz, L., Balkanski, Y., Desboeufs, K., Ebert, M., Kandler, K., Petzold, A., Scheuven, D., Weinbruch, S., and Zhang, D.: Recent progress in understanding physical and chemical properties of African and Asian mineral dust, *Atmos. Chem. Phys.*, 11, 8231–8256, doi:10.5194/acp-11-8231-2011, 2011.
- Freudenthaler, V., Esselborn, M., Wiegner, M., Heese, B., Tesche, M., Ansmann, A., Müller, D., Althausen, A., Wirth, M., and Fix, A.: Depolarization ratio profiling at several wavelengths in pure Saharan dust during SAMUM 2006, *Tellus B*, 61, 165–179, doi:10.1111/j.1600-0889.2008.00396.x, 2009.
- Gama, C., Tchepel, O., Baldasano, J. M., Basart, S., Ferreira, J., Pio, C., Cardoso, J., and Borrego, C.: Seasonal patterns of Saharan dust over Cape Verde—a combined approach using observations and modelling, *Tellus B*, 67, 24410, doi:10.3402/tellusb.v67.24410, 2015.
- Gomes, L., Bergametti, G., Coudé-Gaussen, G., and Rognon, P.: Submicron desert dusts: a sandblasting process, *J. Geophys. Res.*, 95, 13927–13935, doi:10.1029/JD095iD09p13927, 1990.
- Granados-Muñoz, M. J., Navas-Guzmán, F., Bravo-Aranda, J. A., Guerrero-Rascado, J. L., Lyamani, H., Fernández-Gálvez, J., and Alados-Arboledas, L.: Automatic determination of the planetary boundary layer height using lidar: One-year analysis over southeastern Spain, *J. Geophys. Res.*, 117, D18208, doi:10.1029/2012JD017524, 2012.
- Granados-Muñoz, M. J., Guerrero-Rascado, J. L., Bravo-Aranda, J. A., Navas-Guzmán, F., Valenzuela, A., Lyamani, H., Chaikovskiy, A., Wandinger, U., Ansmann, A., Dubovik, O., Grudo, J. O., and Alados-Arboledas, L.: Retrieving aerosol microphysical properties by Lidar-Radiometer Inversion Code (LIRIC) for different aerosol types, *J. Geophys. Res.-Atmos.*, 119, 4836–4858 doi:10.1002/2013JD021116, 2014.
- Granados-Muñoz, M. J., Bravo-Aranda, J. A., Baumgardner, D., Guerrero-Rascado, J. L., Pérez-Ramírez, D., Navas-Guzmán, F., Veselovskii, I., Lyamani, H., Valenzuela, A., Olmo, F. J., Titos, G., Andrey, J., Chaikovskiy, A., Dubovik, O., Gil-Ojeda, M., and Alados-Arboledas, L.: A comparative study of aerosol microphysical properties retrieved from ground-based remote sensing and aircraft in situ measurements during a Saharan dust event, *Atmos. Meas. Tech.*, 9, 1113–1133, doi:10.5194/amt-9-1113-2016, 2016.
- Guerrero-Rascado, J. L., Olmo, F. J., Avilés-Rodríguez, I., Navas-Guzmán, F., Pérez-Ramírez, D., Lyamani, H., and Alados Arboledas, L.: Extreme Saharan dust event over the southern Iberian Peninsula in september 2007: active and passive remote sensing from surface and satellite, *Atmos. Chem. Phys.*, 9, 8453–8469, doi:10.5194/acp-9-8453-2009, 2009.
- Guerrero-Rascado, J. L., Landulfo, E., Antuña, J. C., Barbosa, H. M. J., Barja, B., Bastidas, A. E., Bedoya, A. E., da Costa, R., Estevan, R., Forno, R. N., Gouveia, D. A., Jiménez, C., Larroza, E. G., Lopes, F. J. S., Montilla-Rosero, E., Moreira, G. A., Nakaema, W. M., Nisperuza, D., Otero, L., Pallotta, J. V., Papan-drea, S., Pawelko, E., Quel, E. J., Ristori, P., Rodrigues, P. F., Salvador, J., Sánchez, M. F., and Silva, A.: Towards an instrumental harmonization in the framework of LALINET: dataset of technical specifications, *Proc. SPIE* 2014, Vol. 9246, 924600-1–924600-14, doi:10.1117/12.2066873, 2014.
- Haustein, K., Pérez, C., Baldasano, J. M., Jorba, O., Basart, S., Miller, R. L., Janjic, Z., Black, T., Nickovic, S., Todd, M. C., Washington, R., Müller, D., Tesche, M., Weinzierl, B., Esselborn, M., and Schladitz, A.: Atmospheric dust modeling from meso to global scales with the online NMMB/BSC-Dust model – Part 2: Experimental campaigns in Northern Africa, *Atmos. Chem. Phys.*, 12, 2933–2958, doi:10.5194/acp-12-2933-2012, 2012.
- Heinold, B., Tegen, I., Esselborn, M., Kandler, K., Knippertz, P., Müller, D., Schladitz, A., Tesche, M., Weinzierl, B., Ansmann, A., Althausen, D., Laurent, B., Petzold, A., and Schepanski, K.: Regional Saharan dust modelling during the SAMUM 2006 campaign, *Tellus B*, 61, 307–324, doi:10.1111/j.1600-0889.2008.00387.x, 2009.
- Holben, B. N., Eck, T. F., Slutsker, I., Tanré, D., Buis, J. P., Setzer, A., Vermote, E., Reagan, J. A., Kaufman, Y. J., Nakajima, T., Lavenus, F., Jankowiak, I., and Smirnov, A.: AERONET – A federated instrument network and data archive for aerosol characterization, *Remote Sens. Environ.*, 66, 1–16, 1998.
- Huang, J., Fu, Q., Su, J., Tang, Q., Minnis, P., Hu, Y., Yi, Y., and Zhao, Q.: Taklimakan dust aerosol radiative heating derived from CALIPSO observations using the Fu-Liou radiation model with CERES constraints, *Atmos. Chem. Phys.*, 9, 4011–4021, doi:10.5194/acp-9-4011-2009, 2009.
- IPCC: Contribution of Working Group I to the Fourth Assessment Report of the Intergovernmental Panel on Climate Change, Summary for Policymakers in Climate Change, Cambridge University Press, 2007.
- IPCC: Contribution of Working Group I to the Fifth Assessment Report of the Intergovernmental Panel on Climate Change. Summary for Policymakers in Climate Change, Stocker, Cambridge University Press, 2013.
- Janjic, Z. I., Gerrity Jr, J. P., and Nickovic, S.: An alternative approach to nonhydrostatic modeling, *Mon. Weather Rev.*, 129, 1164–1178, 2001.
- Knoth, O. and Wolke, R.: An explicit-implicit numerical approach for atmospheric chemistry-transport modelling, *Atmos. Environ.*, 32, 1785–1797, 1998.
- Kokkalis, P., Papayannis, A., Mamouri, R. E., Tsaknakis, G., and Amiridis, V.: The EOLE lidar system of the National Technical University of Athens, 629–632, 26th International Laser Radar Conference, 25–29 June 2012, Porto Heli, Greece, 2012.
- Kokkalis, P., Papayannis, A., Amiridis, V., Mamouri, R. E., Veselovskii, I., Kolgotin, A., Tsaknakis, G., Kristiansen, N. I., Stohl, A., and Mona, L.: Optical, microphysical, mass and geometrical properties of aged volcanic particles observed over Athens, Greece, during the Eyjafjallajökull eruption in April 2010 through synergy of Raman lidar and sunphotometer measurements, *Atmos. Chem. Phys.*, 13, 9303–9320, doi:10.5194/acp-13-9303-2013, 2013.
- Kumar, D., Rocadenbosch, F., Sicard, M., Comeron, A., Muñoz, C., Lange, D., Tomás, S., and Gregorio, E.: Six-channel polychromator design and implementation for the UPC elastic/Raman LIDAR, *Proc. SPIE*, 8182, 81820W-1-10, 2011.
- Laurent, B., Tegen, I., Heinold, B., Schepanski, K., Weinzierl, B., and Esselborn, M.: A model study of Saharan dust emissions and distributions during the SAMUM-1 campaign, *J. Geophys. Res.*, 115, D21210, doi:10.1029/2009JD012995, 2010.
- Lelieveld, J., Berresheim, H., Borrmann, S., Crutzen, P. J., Dentener, F. J., Fischer, H., Feichter, J., Flatau, P. J., Heland, J., Holzinger, B., Korrmann, R., Lawrence, M. G., Levin, Z., Markowicz, K. M., Milhalopoulos, N., Minikin, A., Ramanathan, V., de Reus, M., Roelofs, G. J., Scheeren, H. A., Sciare, J.,

- Schlager, H., Schultz, M., Siegmund, P., Steil, B., Stephanou, E. G., Stier, P., Traub, M., Warneke, C., Williams, J., and Ziereis, H.: Global air pollution crossroads over the Mediterranean, *Science*, 298, 794–799, 2002.
- Lopatin, A., Dubovik, O., Chaikovskiy, A., Goloub, P., Lapyonok, T., Tanré, D., and Litvinov, P.: Enhancement of aerosol characterization using synergy of lidar and sun-photometer coincident observations: the GARRLiC algorithm, *Atmos. Meas. Tech.*, 6, 2065–2088, doi:10.5194/amt-6-2065-2013, 2013.
- Lyamani, H., Valenzuela, A., Perez-Ramirez, D., Toledano, C., Granados-Muñoz, M. J., Olmo, F. J., and Alados-Arboledas, L.: Aerosol properties over the western Mediterranean basin: temporal and spatial variability, *Atmos. Chem. Phys.*, 15, 2473–2486, doi:10.5194/acp-15-2473-2015, 2015.
- Mamouri, R. E. and Ansmann, A.: Fine and coarse dust separation with polarization lidar, *Atmos. Meas. Tech.*, 7, 3717–3735, doi:10.5194/amt-7-3717-2014, 2014.
- Mattis, I., Ansmann, A., Müller, D., Wandinger, U., and Althausen, D.: Multiyear aerosol observations with dual-wavelength Raman lidar in the framework of EARLINET, *J. Geophys. Res.*, 109, D13203, doi:10.1029/2004JD004600, 2004.
- McCormick, M. P., Wang, P. H., and Poole, L. R.: Stratospheric aerosols and clouds, in: *Aerosol-Cloud-Climate Interactions*, edited by: Hobbs, P. V., Academic Press, 205–222, 1993.
- Nabat, P., Somot, S., Mallet, M., Sanchez-Lorenzo, A., and Wild, M.: Contribution of anthropogenic sulfate aerosols to the changing Euro-Mediterranean climate since 1980, *Geophys. Res. Lett.*, 41, 5605–5611, doi:10.1002/2014GL060798, 2014.
- Nabat, P., Somot, S., Mallet, M., Sevault, F., Chiacchio, M., and Wild, M.: Direct and semi-direct aerosol radiative effect on the Mediterranean climate variability using a coupled regional climate system model, *Clim. Dynam.*, 44, 1127–1155, doi:10.1007/s00382-014-2205-6, 2015.
- Nakajima, T., Tonna, G., Rao, R., Boi, P., Kaufman, Y., and Holben, B.: Use of sky brightness measurements from ground for remote sensing of particulate polydispersions, *Appl. Optics*, 35, 2672–2686, doi:10.1364/AO.35.002672, 1996.
- Nemuc, A., Vasilescu, J., Talianu, C., Belegante, L., and Nicolae, D.: Assessment of aerosol's mass concentrations from measured linear particle depolarization ratio (vertically resolved) and simulations, *Atmos. Meas. Tech.*, 6, 3243–3255, doi:10.5194/amt-6-3243-2013, 2013.
- Nickovic, S., Kallos, K., Papadopoulos, A., and Kakaliagou, O.: A model for prediction of desert dust cycle in the atmosphere, *J. Geophys. Res.*, 106, 18113–18118, doi:10.1029/2000JD900794, 2001.
- Noh, Y. M.: Single-scattering albedo profiling of mixed Asian dust plumes with multiwavelength Raman lidar, *Atmos. Environ.*, 95, 305–317, doi:10.1016/j.atmosenv.2014.06.028, 2014.
- Olmo, F. J., Quirantes, A., Alcántara, A., Lyamani, H., and Alados-Arboledas, L.: Preliminary results of a non-spherical aerosol method for the retrieval of the atmospheric aerosol optical properties, *J. Quant. Spectrosc. Ra.*, 100, 305–314, doi:10.1016/j.jqsrt.2005.11.047, 2006.
- Papayannis, A., Amiridis, V., Mona, L., Tsaknakis, G., Balis, D., Bösenberg, J., Chaikovskiy, A., De Tomasi, F., Grigorov, I., Mattis, I., Mitev, V., Müller, D., Nickovic, S., Pérez, C., Pietruczuk, A., Pisani, G., Ravetta, F., Rizi, V., Sicard, M., Trickl, T., Wiegner, M., Gerding, M., Mamouri, R. E., D'Amico, G., and Pappalardo, G.: Systematic lidar observations of Saharan dust over Europe in the frame of EARLINET (2000–2002), *J. Geophys. Res.*, 113, D10204, doi:10.1029/2007JD009028, 2008.
- Papayannis, A., Nicolae, D., Kokkalis, P., Biniotoglou, I., Talianu, C., Belegante, L., Tsaknakis, G., Cazacu, M. M., Vetres, I., and Ilic, L.: Optical, size and mass properties of mixed type aerosols in Greece and Romania as observed by synergy of lidar and sunphotometers in combination with model simulations: A case study, *Sci. Total Environ.*, 500–501, 277–294, doi:10.1016/j.scitotenv.2014.08.101, 2014.
- Pappalardo, G., Amodeo, A., Apituley, A., Comeron, A., Freudenthaler, V., Linné, H., Ansmann, A., Bösenberg, J., D'Amico, G., Mattis, I., Mona, L., Wandinger, U., Amiridis, V., Alados-Arboledas, L., Nicolae, D., and Wiegner, M.: EARLINET: towards an advanced sustainable European aerosol lidar network, *Atmos. Meas. Tech.*, 7, 2389–2409, doi:10.5194/amt-7-2389-2014, 2014.
- Pérez, C., Nickovic, S., Pejanovic, G., Baldasano, J. M., and Özsoy, E.: Interactive dust-radiation modeling: A step to improve weather forecasts, *J. Geophys. Res.*, 111, D16206, doi:10.1029/2005JD006717, 2006a.
- Pérez, C., Nickovic, S., Baldasano, J. M., Sicard, M., Rocadenbosch, F., and Cachorro, V. E.: A long Saharan dust event over the western Mediterranean: Lidar, Sun photometer observations, and regional dust modeling?, *J. Geophys. Res.*, 111, D15214, doi:10.1029/2005JD006579, 2006b.
- Pérez, C., Haustein, K., Janjic, Z., Jorba, O., Huneus, N., Baldasano, J. M., Black, T., Basart, S., Nickovic, S., Miller, R. L., Perlwitz, J. P., Schulz, M., and Thomson, M.: Atmospheric dust modeling from meso to global scales with the online NMMB/BSC-Dust model – Part 1: Model description, annual simulations and evaluation, *Atmos. Chem. Phys.*, 11, 13001–13027, doi:10.5194/acp-11-13001-2011, 2011.
- Pérez-Ramírez, D., Navas-Guzmán, F., Lyamani, H., Fernández-Gálvez, J., Olmo, F. J., and Alados-Arboledas, L.: Retrievals of precipitable water vapor using star photometry: Assessment with Raman lidar and link to sun photometry, *J. Geophys. Res.*, 117, D05202, doi:10.1029/2011JD016450, 2012.
- Perrone, M. R., De Tomasi, F., and Gobbi, G. P.: Vertically resolved properties by multi-wavelength lidar measurements, *Atmos. Chem. Phys.*, 14, 1185–1204, doi:10.5194/acp-14-1185-2014, 2014.
- Preißler, J., Wagner, F., Pereira, S. N., and Guerrero-Rascado, J. L.: Multi-instrumental observation of an exceptionally strong Saharan dust outbreak over Portugal, *J. Geophys. Res.*, 116, D24204, doi:10.1029/2011JD016527, 2011.
- Remer, L. A., Kaufman, Y. J., Tanré, D., Mattoo, S., Chu, D. A., Martins, J. V., Li, R. R., Ichoku, C., Levy, R. C., Kleidman, R. G., Eck, T. F., Vermote, E., and Holben, B. N.: The MODIS aerosol algorithm, products, and validation, *J. Atmos. Sci.*, 62, 947–973, 2005.
- Rodríguez, S., Alastuey, A., Alonso-Pérez, S., Querol, X., Cuevas, E., Abreu-Afonso, J., Viana, M., Pérez, N., Pandolfi, M., and de la Rosa, J.: Transport of desert dust mixed with North African industrial pollutants in the subtropical Saharan Air Layer, *Atmos. Chem. Phys.*, 11, 6663–6685, doi:10.5194/acp-11-6663-2011, 2011.
- Schättler, U., Doms, G., and Schraff, C.: A Description of the Non-hydrostatic Regional COSMO-Model, Deutscher Wetterdienst,

- Offenbach, available at: <http://www.cosmo-model.org> (last access: 23 May 2016), 2008.
- Schepanski, K., Tegen, I., Laurent, B., Heinold, B., and Macke, A.: A new Saharan dust source activation frequency map derived from MSG-SEVIRI IR-channels, *Geophys. Res. Lett.*, 34, L18803, doi:10.1029/2007GL030168, 2007.
- Schepanski, K., Tegen, I., and Macke, A.: Saharan dust transport and deposition towards the tropical northern Atlantic, *Atmos. Chem. Phys.*, 9, 1173–1189, doi:10.5194/acp-9-1173-2009, 2009.
- Shimizu, A., Sugimoto, N., Matsui, I., Arao, K., Uno, I., Murayama, T., Kagawa, N., Aoki, K., Uchiyama, A., and Yamazaki, A.: Continuous observations of Asian dust and other aerosols by polarization lidars in China and Japan during ACE-Asia, *J. Geophys. Res.*, 109, D19S17, doi:10.1029/2002JD003253, 2004.
- Sicard, M., D'Amico, G., Comerón, A., Mona, L., Alados-Arboledas, L., Amodeo, A., Baars, H., Baldasano, J. M., Belegante, L., Biniotoglou, I., Bravo-Aranda, J. A., Fernández, A. J., Fréville, P., García-Vizcaíno, D., Giunta, A., Granados-Muñoz, M. J., Guerrero-Rascado, J. L., Hadjimitsis, D., Haeferle, A., Hervo, M., Iarlori, M., Kokkalis, P., Lange, D., Mamouri, R. E., Mattis, I., Molero, F., Montoux, N., Muñoz, A., Muñoz Porcar, C., Navas-Guzmán, F., Nicolae, D., Nisantzi, A., Papagiannopoulos, N., Papayannis, A., Pereira, S., Preißler, J., Pujadas, M., Rizi, V., Rocadenbosch, F., Sellegri, K., Simeonov, V., Tsaknakis, G., Wagner, F., and Pappalardo, G.: EARLINET: potential operationality of a research network, *Atmos. Meas. Tech.*, 8, 4587–4613, doi:10.5194/amt-8-4587-2015, 2015.
- Sokolik, I. N. and Toon, O. B.: Incorporation of mineralogical composition into models of the radiative properties of mineral aerosol from UV to IR wavelengths, *J. Geophys. Res.*, 104, 9423–9444, 1999.
- Takamura, T. and Nakajima, T.: Overview of SKYNET and its activities, *Opt. Pura Apl.*, 37, 3303–3308, 2004.
- Tegen, I. and Lacis, A. A.: Modeling of particle size distribution and its influence on the radiative properties of mineral dust aerosol, *J. Geophys. Res.*, 101, 19–237, 1996.
- Tegen, I., Schepanski, K., and Heinold, B.: Comparing two years of Saharan dust source activation obtained by regional modelling and satellite observations, *Atmos. Chem. Phys.*, 13, 2381–2390, doi:10.5194/acp-13-2381-2013, 2013.
- Tsekeri, A., Amiridis, V., Kokkalis, P., Basart, S., Chaikovsky, A., Dubovik, O., Papayannis, A., Baldasano, J. M., and Gross, B.: Application of a synergetic lidar and sunphotometer algorithm for the characterization of a dust event over Athens, Greece, *British J. Environ. Clim. Change*, 3, 531–546, doi:10.9734/BJECC/2013/2615, 2013.
- Valenzuela, A., Olmo, F. J., Lyamani, H., Antón, M., Quirantes, A., and Alados-Arboledas, L.: Classification of aerosol radiative properties during African desert dust intrusions over southeastern Spain by sector origins and cluster analysis, *J. Geophys. Res.*, 117, D06214, doi:10.1029/2011JD016885, 2012.
- Valenzuela, A., Olmo, F. J., Lyamani, H., Granados-Muñoz, M. J., Antón, M., Guerrero-Rascado, J. L., Quirantes, A., Toledano, C., Perez-Ramírez, D., and Alados-Arboledas, L.: Aerosol transport over the western Mediterranean basin: Evidence of the contribution of fine particles to desert dust plumes over Alborán Island, *J. Geophys. Res.*, 119, 14028–14044, doi:10.1002/2014JD022044, 2014.
- Vukovic, A., Vujadinovic, M., Pejanovic, G., Andric, J., Kumjian, M. R., Djurdjevic, V., Dacic, M., Prasad, A. K., El-Askary, H. M., Paris, B. C., Petkovic, S., Nickovic, S., and Sprigg, W. A.: Numerical simulation of “an American haboob”, *Atmos. Chem. Phys.*, 14, 3211–3230, doi:10.5194/acp-14-3211-2014, 2014.
- Wagner, J., Ansmann, A., Wandinger, U., Seifert, P., Schwarz, A., Tesche, M., Chaikovsky, A., and Dubovik, O.: Evaluation of the Lidar/Radiometer Inversion Code (LIRIC) to determine microphysical properties of volcanic and desert dust, *Atmos. Meas. Tech.*, 6, 1707–1724, doi:10.5194/amt-6-1707-2013, 2013.
- Wang, Y., Sartelet, K. N., Bocquet, M., Chazette, P., Sicard, M., D'Amico, G., Léon, J. F., Alados-Arboledas, L., Amodeo, A., Augustin, P., Bach, J., Belegante, L., Biniotoglou, I., Bush, X., Comerón, A., Delbarre, H., García-Vizcaino, D., Guerrero-Rascado, J. L., Hervo, M., Iarlori, M., Kokkalis, P., Lange, D., Molero, F., Montoux, N., Muñoz, A., Muñoz, C., Nicolae, D., Papayannis, A., Pappalardo, G., Preissler, J., Rizi, V., Rocadenbosch, F., Sellegri, K., Wagner, F., and Dulac, F.: Assimilation of lidar signals: application to aerosol forecasting in the western Mediterranean basin, *Atmos. Chem. Phys.*, 14, 12031–12053, doi:10.5194/acp-14-12031-2014, 2014.
- Welton, E. J., Campbell, J. R., Berkoff, T. A., Valencia, S., Spinhirne, J. D., Holben, B., and Tsay, S. C.: 5.2 The Nasa Micro-Pulse Lidar Network (MPLNET): co-location of lidars with AERONET sunphotometers and related Earth Science applications, *Proc. 85th Annu. Meet. Am. Meteor. Soc.*, San Diego, 9–13 January, 5165–5169, 2005.
- Wolke, R., Schroeder, W., Schroedner, R., and Renner, E.: Influence of grid resolution and meteorological forcing on simulated European air quality: A sensitivity study with the modeling system COSMO-MUSCAT, *Atmos. Environ.*, 53, 110–130, doi:10.1016/j.atmosenv.2012.02.085, 2012.